Journal of Vertebrate Paleontology

Postcranial anatomy and osteoderm histology of *Riojasuchus tenuisceps* and a phylogenetic update on Ornithosuchidae (Archosauria, Pseudosuchia)

M. Belén von Baczko, Julia B. Desojo & Denis Ponce

View supplementary material

Published online: 05 Feb 2020.

Submit your article to this journal

View related articles

View Crossmark data

ARTICLE

POSTCRANIAL ANATOMY AND OSTEODERM HISTOLOGY OF *RIOJASUCHUS TENUISCEPS* AND A PHYLOGENETIC UPDATE ON ORNITHOSUCHIDAE (ARCHOSAURIA, PSEUDOSUCHIA)

M. BELÉN VON BACZKO, [*,1,2] JULIA B. DESOJO, [1,2] and DENIS PONCE[2,3,4]

[1]División Paleontología de Vertebrados, Museo de La Plata, Paseo del Bosque s/n (B1900FWA), La Plata, Buenos Aires, Argentina, belenvonbaczko@gmail.com;

[2]Consejo Nacional de Investigaciones Científicas y Técnicas (CONICET), Godoy Cruz 2290 (C1425FQB), Ciudad Autónoma de Buenos Aires, Argentina, julideso@fcnym.unlp.edu.ar;

[3]Instituto de Investigación en Paleobiología y Geología (IIPG), Universidad Nacional de Río Negro, Av. Roca 1242, 8332, General Roca, Río Negro, Argentina, denispunrn@yahoo.com.ar;

[4]Museo 'Carlos Ameghino,' Belgrano 1700, Paraje Pichi Ruca (predio Marabunta), 8300, Cipolletti, Río Negro, Argentina

ABSTRACT—Ornithosuchidae is a group of terrestrial quadrupedal pseudosuchian archosaurs from the Late Triassic of South America and Europe. *Riojasuchus tenuisceps* is arguably one of the best representative species of this clade because it comprises very well-preserved three-dimensional, almost complete skeletons. However, *R. tenuisceps* was originally described 50 years ago and compared then only with *Ornithosuchus woodwardi* and their affinities were discussed in detail. Here, we provide a detailed description of the postcranial skeleton of *R. tenuisceps*, which exhibits several remarkable features within pseudosuchians. When a wide spectrum of pseudosuchian archosaurs are considered, the alleged character that linked ornithosuchids with dinosaurs resulted in convergences and some were registered in other pseudosuchian groups as well. *Riojasuchus tenuisceps* also provided crucial information about the 'crocodile-reversed' tarsus, which is a unique feature of ornithosuchids, but it is not completely preserved in *O. woodwardi* and it is unknown in *Venaticosuchus rusconii*. In addition, the first histological analysis of cervical and dorsal osteoderms of *R. tenuisceps* was carried out as well, in order to test the utility of these structures as skeletochronological tools. Finally, the phylogenetic context of Ornithosuchidae is discussed based on the latest phylogenetic studies, which show a close affinity with Erpetosuchidae.

SUPPLEMENTAL DATA—Supplemental materials are available for this article for free at www.tandfonline.com/UJVP

INTRODUCTION

Ornithosuchids are an unusual and rather poorly known group of pseudosuchian archosaurs registered in Upper Triassic continental deposits of South America and Europe. Ornithosuchids are found alongside with erpetosuchids, aetosaurs, loricatans, gracilisuchids, and basal crocodylomorphs (Nesbitt, 2011; Butler et al., 2014; Ezcurra et al., 2017). They are terrestrial quadrupedal to facultatively bipedal animals, with medium body sizes of ca. 2 m in length and scavenger feeding habits (Benton, 1983; Baczko, 2018). This group is distinguished by a bizarre cranial morphology (downturned premaxilla, two-tooth diastema, palatine-pterygoid fenestra, mandible shorter than skull) and several controversial postcranial features (perforated acetabulum, rotated femoral head, crocodile-reversed ankle joint) that turned them into a phylogenetic riddle for decades (Sereno, 1991; Baczko and Ezcurra, 2013; Baczko and Desojo, 2016).

Ornithosuchidae is currently composed of three species from present-day Argentina and Scotland: *Riojasuchus tenuisceps* (Los Colorados Formation, middle Norian), *Venaticosuchus rusconii* (Ischigualasto Formation, late Carnian–early Norian), and *Ornithosuchus woodwardi* (Lossiemouth Sandstones Formation, late Carnian–early Norian). *Riojasuchus tenuisceps*, particularly, was discovered at the Quebrada de Los Jachalleros locality, La Rioja, northwestern Argentina, and formed part of the Coloradian fauna, a very rich and diverse assemblage of Late Triassic tetrapods, composed of ornithosuchids, basal loricatans, sphenosuchians, protosuchians, sauropodomorphs, theropods, quelonids, and cynodonts (Bonaparte, 1973; Arcucci et al., 2004). *Riojasuchus tenuisceps* includes four specimens of similar size, three of whom are very well preserved, and together represent almost the complete skeleton of this species, which provides crucial information about the anatomy of this peculiar archosaur. *Riojasuchus* was originally described by Bonaparte (1972) highlighting its similarities to *Ornithosuchus woodwardi* (= *Ornithosuchus 'longidens'*; see Baczko and Ezcurra, 2016), the best-known ornithosuchid at that time, although its affinities were quite unclear by then.

Despite Ornithosuchidae being a small group with only three species known, some aspects of these species need to be studied in detail. As a continuation of the recently published description of the skull and cranial endocast of *Riojasuchus tenuisceps*, we provide here a detailed description of the postcranial skeleton, based on firsthand study of all known specimens. Additionally, a histological analysis of its cervical and dorsal osteoderms was carried out to document the microanatomy of *Riojasuchus*. The phylogenetic position of Ornithosuchidae is also discussed

---

*Corresponding author.

Color versions of one or more of the figures in the article can be found online at www.tandfonline.com/ujvp.

based on the latest analyses that revealed their close affinity with the clade Erpetosuchidae.

HORIZON AND LOCALITY

Upper beds of the Los Colorados Formation (Late Triassic), Quebrada de los Jachalleros, General Lavalle, La Rioja, northwestern Argentina (Fig. 1). This upper section of the Los Colorados Formation has yielded a particular fauna named the 'Coloradian' ('Coloradense'), which is mainly composed of pseudosuchians (ornithosuchids, aetosaurs, rauisuchians, and crocodylomorphs), avemetatarsalians (sauropodomorphs and theropods), quelonids, and cynodonts. The latest radioisotopic and paleomagnetic studies dated the Coloradian strata at 227–213 Ma, corresponding to a late Norian age (Kent et al., 2014).

Institutional Abbreviations—**SNSB-BSPG**, Bayerische Staatssammlung für Paläontologie und Geologie, Munich, Germany; **CRILAR-Pv**, Paleontología de Vertebrados, Centro Regional de Investigaciones Científicas y Transferencia Tecnológica, Anillaco, Argentina; **GPIT**, Institut für Geowissenschaften, Universität Tübingen, Tübingen, Germany; **MACN-He**, Colección Nacional de Herpetología, Museo Argentino de Ciencias Naturales Bernardino Rivadavia, Buenos Aires, Argentina; **NHMUK**, Natural History Museum, London, U.K.; **PULR**, Museo de Paleontología, Universidad Nacional de La Rioja, La Rioja, Argentina; **PVL**, Paleontología de Vertebrados, Instituto Miguel Lillo, Tucumán, Argentina; **SAM-PK**, Iziko South African Museum, Cape Town, South Africa; **SMNS**, Staatliches Museum für Naturkunde Stuttgart, Stuttgart, Germany; **TMM**, Texas Memorial Museum, Austin, Texas, U.S.A.; **TTU**, Texas Tech University Museum, Lubbock, Texas, U.S.A.; **UCMP**, University of California Museum of Paleontology, Berkeley, California, U.S.A.; **UFRGS-PV**, Universidade Federal do Rio Grande do Sul, Porto Alegre, Brazil.

MATERIALS AND METHODS

Riojasuchus tenuisceps is currently represented by four specimens, PVL 3827 (holotype), PVL 3814, PVL 3826, and PVL 3828, three of which represent almost the complete skeleton (Fig. 2). All specimens were studied firsthand at the Instituto Miguel Lillo, where they are accessioned. No specimens were purchased or donated for the purpose of this study. Measurements were made with a digital caliper set with a maximum deviation of 0.02 mm, but measurements were rounded to the nearest 0.1 mm.

For the histological study, three transverse sections were made, one from a cervical osteoderm and two from a dorsal osteoderm of *Riojasuchus tenuisceps* (PVL 3814), and analyzed. Given the destructive nature of the procedure for obtaining thin sections, the sampled elements were photographed and measured before processing. Also, a cast of each osteoderm was made to avoid the loss of morphological information. The specimens were sectioned following the methodology of Chinsamy and Raath (1992). The histological sections were made in the Departamento de Geología of Universidad Nacional de San Luis, Argentina. The sections were analyzed under a petrographic microscope (Nikon E200 Pol and Zeiss Imager.A2m) under plane- and cross-polarized light. We use the term 'external' to refer to the portion of the osteoderm oriented toward the body surface and the term 'basal' for the portion that is oriented toward the interior of the organism (Scheyer and Sander, 2004). These terms are synonyms of 'distal/proximal' (Main et al., 2005) or 'superficial/deep' (Hill and Lucas, 2006; Hill, 2010). In addition, we use the term 'marginal' cortex to refer to the lateral and medial regions of the osteoderms. For the terminology of growth marks, we follow the nomenclature proposed by Francillon-Vieillot et al. (1990).

For the phylogenetic analyses, we augmented the data matrices of Ezcurra et al. (2017) and Lacerda et al. (2018), which are available as Supplemental Data 1 and 2, respectively. Changes made to the codings of characters in these matrices are summarized in Supplemental Data 3.

SYSTEMATIC PALEONTOLOGY

ARCHOSAURIA Cope, 1869, sensu Gauthier and Padian, 1985
PSEUDOSUCHIA Zittel, 1887–1890, sensu Gauthier and Padian, 1985
ORNITHOSUCHIDAE Huene, 1908, sensu Sereno, 1991
RIOJASUCHUS Bonaparte, 1967
RIOJASUCHUS TENUISCEPS Bonaparte, 1967
(Figs. 2–14)

Holotype—PVL 3827, a very well-preserved skull with postcranial elements. The skull has the right hemimandible articulated, but the left hemimandible was disarticulated during the original preparation. The skeleton comprises 26 partially articulated vertebrae (19 presacrals, three sacrals, and four caudals) with articulated paramedial osteoderms in some cervical and dorsal regions, incomplete scapulae and coracoids, incomplete humeri, a distal portion of left radius and ulna articulating with carpus, left ilium and pubis, left femur, left tibia and fibula articulating with complete pes, and partial right pes.
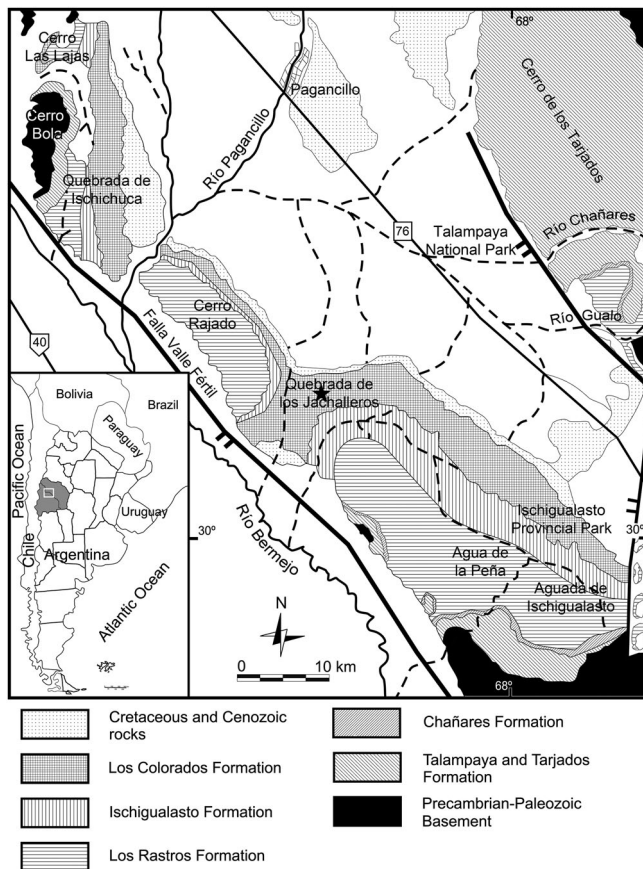

FIGURE 1. Geological map of the Los Colorados Formation, Ischigualasto-Villa Unión Basin, La Rioja, Argentina. Star indicates the location where the specimens were collected. Modified from Baczko and Desojo (2016).
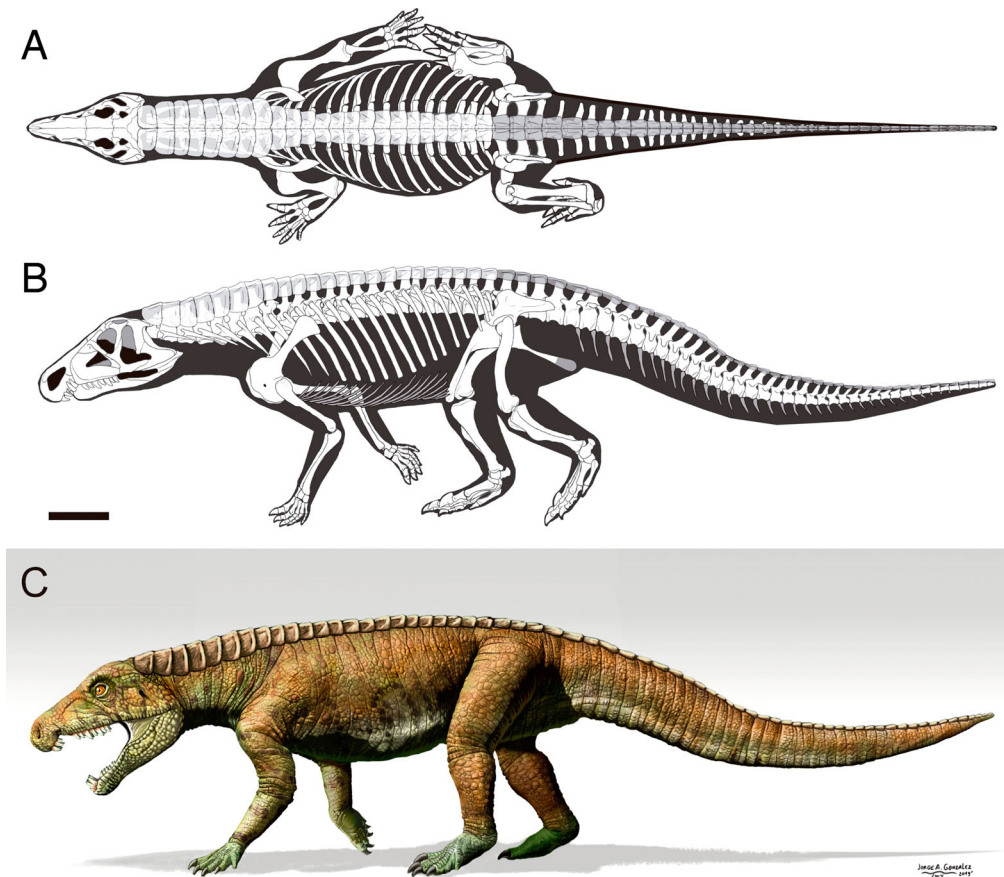
FIGURE 2. *Riojasuchus tenuisceps*, skeletal reconstruction in **A**, dorsal and **B**, lateral views. **C**, life reconstruction of *Riojasuchus tenuisceps* by Jorge Gonzalez. Scale bar equals 10 cm.

Referred Material—PVL 3828, an almost complete skull with postcranial elements. The skull has some incomplete elements such as the premaxillae, nasals, left jugal and lacrimal, squamosals, left surangular, and right angular and articular. Both hemimandibles are articulated and occluded. The skeleton is constituted of several skeletal elements, including 32 partially articulated vertebrae (19 preasacrals, three sacrals, and 13 caudals); incomplete scapulae and coracoids, humeri, radii, and ulnae; left ilium and a fragmentary ischium; left femur; incomplete right femur; incomplete tibiae; fragmentary right fibula; isolated left 4th distal tarsal; left calcaneum; and several disarticulated phalanges.

PVL 3826, consisting of 28 partly articulated vertebrae (19 presacrals and nine caudals), two fragmentary scapulae and coracoids, right humerus, fragmentary radius and ulna, incomplete right ilium, distal end of left femur, and fragmentary tibia.

PVL 3814, consisting of several isolated poorly preserved vertebrae, fragmentary left humerus, fragmentary tibia, and several isolated paramedial osteoderms.

Comment—Bonaparte (1972) indicated that the assignment of some elements to each of the four specimens of *Riojasuchus* is arguable because they were found close together and their sizes are even. For example, he affirmed that the two left ilia and the fragment from the right ilium known for *Riojasuchus* were not in articulation and therefore cannot be assigned to any of the four specimens with certainty. For that reason, we would like to point out that the original assignment of these elements was arbitrary. However, the left ilium assigned to the holotype is dorsoventrally deformed, and the same kind of deformation can be recognized in its left femur. In contrast, the left ilium assigned to PVL 3828 does not exhibit postmortem deformation, which is consistent with the left femur of the same specimen. Following this reasoning, the original arbitrary assignment of both left ilia by Bonaparte (1967) seems adequate and is not modified here. Concerning the incomplete right ilium of PVL 3826, this fragmentary element is not deformed and could correspond to either PVL 3828 or PVL 3826. Moreover, the sacral vertebrae of PVL 3828 do not preserve the sacral ribs; therefore, it is impossible to test whether it articulated with this ilium or not. And on the other hand, only the last sacral of PVL 3826 is poorly preserved, but the fragmentary ilium is represented by its anterior portion and does not articulate with the last sacral at all. Therefore, the assignment of the right ilium cannot be confirmed or rebutted, because there is no evidence against the original assignment, and we opt not to modify it.

Diagnosis—*Riojasuchus tenuisceps* is distinguished from all other archosaurs by the combination of the following characters (autapomorphies noted with asterisk): (1) strongly downturned premaxilla; (2) three premaxillary teeth; (3) seven maxillary teeth; (4) second and third teeth on dentary hypertrophied; (5) two-tooth diastema between premaxilla and maxilla; (6) deep antorbital fossa with the anterior and ventral edges almost coinciding with the same edges of the maxilla itself*; (7) nasal-prefrontal contact absent; (8) jugal with vertical process separating

antorbital fenestra from infratemporal fenestra; (9) orbit with ventral point surrounded by 'V'-shaped dorsal processes of the jugal; (10) suborbital fenestra equal in size to the palatine-pterygoid fenestra*; (11) posterolateral process of the parietals anteriorly inclined greater than 45°; (12) reduced supratemporal fenestra; (13) 'L'-shaped infratemporal fenestra; (14) presence of a palatine-pterygoid fenestra; (15) lower jaws shorter than skull length; (16) presence of a first small tooth anterior to the two hypertrophied teeth; (17) anterior end of the dentary dorsally expanded; (18) dentary-splenial symphysis present along one-third of the lower jaw; (19) sharp surangular shelf; (20) presence of a surangular foramen; (21) atlantal neural arch bases contact at the midline*; (22) ventral keel of cervical vertebrae extends ventral to the central rims; (23) pubis longer than 70% of femoral length; (24) anterior trochanter (= M. iliofemoralis cranialis insertion) forms a steep margin with the shaft but is completely connected to the shaft; (25) ventral astragalocalcanear articular surface concavoconvex with concavity on astragalus; and (26) metatarsal V without 'hooked' proximal end.

RESULTS

Axial Skeleton

Proatlas—It is composed of two dorsoventrally compressed slits of bone slightly curved lateroventrally (Fig. 3A); they contact each other medially, constituting the roof of the neural canal (PVL 3827). The proatlas is barely anteroposteriorly expanded on its lateral edge.

Atlas—It has a subquadrangular centrum in posterior view, with deeply concave anterior and posterior articular facets for the articulation of the occipital condyle and the axis, respectively (PVL 3826; Fig. 3C–E). The lateral surfaces of the centrum are slightly concave, and the ventral surface has a marked concavity and no hypapophyses. The postzygapophyses are posteriorly projected; they are subtriangular in dorsal view, being laterally expanded anteriorly and tapering posteriorly; their articular facets are ventrally directed (Fig. 3E). The base of the neural arches of the atlas contact medially (Fig. 3A, B, D), which, according to Sereno (1991), is considered an autapomorphic character for *Riojasuchus tenuisceps*, but this feature is also present in modern crocodiles such as *Crocodylus novaguinea* (SMNS 6664) and *Osteolaemus tetraspis* (SMNS 6665).

Axis—It is the longest element of the axial series, and its centrum is laterally compressed, being half its maximum width. It has a well-developed hypapophysis at the midline of its ventral surface, although it is partially broken in some regions in PVL 3827 and PVL 3828 (Fig. 3A, B). The axis is articulated within the vertebral series; therefore, its anterior and posterior articular facets cannot be seen in PVL 3827 and PVL 3828. The ventral margin of the anterior articular surface is wider than the posterior one, and it is markedly curved. The diapophyses and parapophyses of the axis cannot be clearly recognized on any specimen of *R. tenuisceps* (PVL 3827, PVL 3828), but the corresponding cervical ribs are preserved in articulation with the axis of the holotype (Fig. 3A, B). The neural spine of the axis of *R. tenuisceps* is anteroposteriorly expanded, reaching the anterior margin of the atlas anteriorly and the middle region of the third cervical vertebra posteriorly. The external surface of the spine is striated at its base (PVL 3828), possibly for the insertion of the neck muscles (M. interarticularis and M. epistropheo capitis; Tsuihiji, 2005). The prezygapophyses of the axis are completely covered by the postzygapophyses of the atlas in both PVL 3827 and PVL 3828. Their anterior extent and articular facets cannot be seen in any these specimens. The postzygapophyses are elongated and posterolaterally projected, extending posterior to the posterior margin of the centrum (Fig. 3A). These were also

preserved in articulation with the third cervical vertebra, and their articular facets cannot be observed.

Postaxial Cervical Vertebrae—These correspond to the region between the third and tenth vertebrae (C3–C10), although the posterior cervical vertebrae are difficult to differentiate from the anterior dorsal vertebrae. The centra of the postaxial cervical vertebrae of *R. tenuisceps* are as long as high in all the series, becoming slightly shorter toward the posterior ones. The anterior and posterior articular facets are round, approximately as high as long, and concave (amphicoelic). The middle region of the centra is compressed, granting the cervical vertebrae a spool shape, although these centra are less compressed than the axis centrum. There are no lateral fossae or accessory laminae between the apophyses, nor between the apophyses and the centrum. There is no evidence of the presence of a hyposphene or a hypanthrum in any specimen of *R. tenuisceps*. The ventral surface of the cervical centra has a well-developed hypapophysis (ventral keel) that becomes anteroposteriorly longer and dorsoventrally higher toward the middle cervical vertebrae, reaching its largest development at the C5 (Fig. 3A, B). The hypapophysis of the posterior cervical vertebrae is much shorter, occupying only the anterior half of the centrum and becoming lower toward the last cervical vertebrae and being almost imperceptible at the C10 (PVL 3827) (Fig. 4A, B).

The diapophyses of the postaxial cervical vertebrae of *R. tenuisceps* can be recognized as a small ventrolateral projection on each side of the centrum located ventral to the neurocentral suture. These diapophyses are very short on the first postaxial cervical vertebrae but are longer toward the posterior ones; their relative position changes toward the posterior cervical vertebrae (C7–C10), being located on top of the neurocentral suture. The parapophyses can be identified from C4 (PVL 3828) on the anterior margin of the centrum, below the dorsoventral midline (Figs. 3A, B, F, G, 4A–D). The parapophyses are short; they are laterally projected on the anterior cervical vertebrae (PVL 3828: C4–C6) and posterolaterally projected on the posterior cervical vertebrae (PVL 3827: C7–C10). On the last cervical vertebra (PVL 3827: C10), the parapophyses are located at the dorsoventral midline of the centrum and are dorsoventrally expanded, resembling the condition of the first dorsal vertebrae, but without contacting the neurocentral suture as in the latter (PVL 3827: D1).

The neural spines of the postaxial cervical vertebrae are located on the posterior margin of the centra; they are as high as the centra and anteroposteriorly short. They are dorsoventrally oriented and widen abruptly on their apical end, forming a well-defined spine table (Fig. 3F). The spine tables of the postaxial cervical vertebrae of *R. tenuisceps* are rectangular in dorsal view, being approximately three times wider than anteroposteriorly long and triple the width of its base (PVL 3827: C7–C8). The dorsal surface of the spine tables is flat, whereas that of erpetosuchids is concave (*Tarjadia ruthae*: CRILAR-Pv 478).

The prezygapophyses of the postaxial cervical vertebrae are anterolaterally oriented, barely extending beyond to the anterior margin of the centrum (Fig. 3G), whereas the postzygapophyses are posterolaterally oriented and extending entirely posterior to the posterior margin of the centrum. The articular facets of the prezygapophyses can only be seen in a couple of vertebrae (PVL 3827: C8, PVL 3828: C6); these facets are oval and dorsomedially oriented at 45° from the horizontal plane. The postzygapophyses are either in articulation or severely damaged; therefore, their preservation does not allow the observation of any detail of their articular facets (Fig. 3F, G).

Dorsal Vertebrae—These are better preserved in the holotype (PVL 3827) than in the referred materials. In the holotype, they were preserved in two articulated sections plus two isolated posterior dorsal vertebrae. These sections were here identified as the first three dorsal vertebrae articulated with the two last cervical vertebrae and their corresponding ribs, and the other section
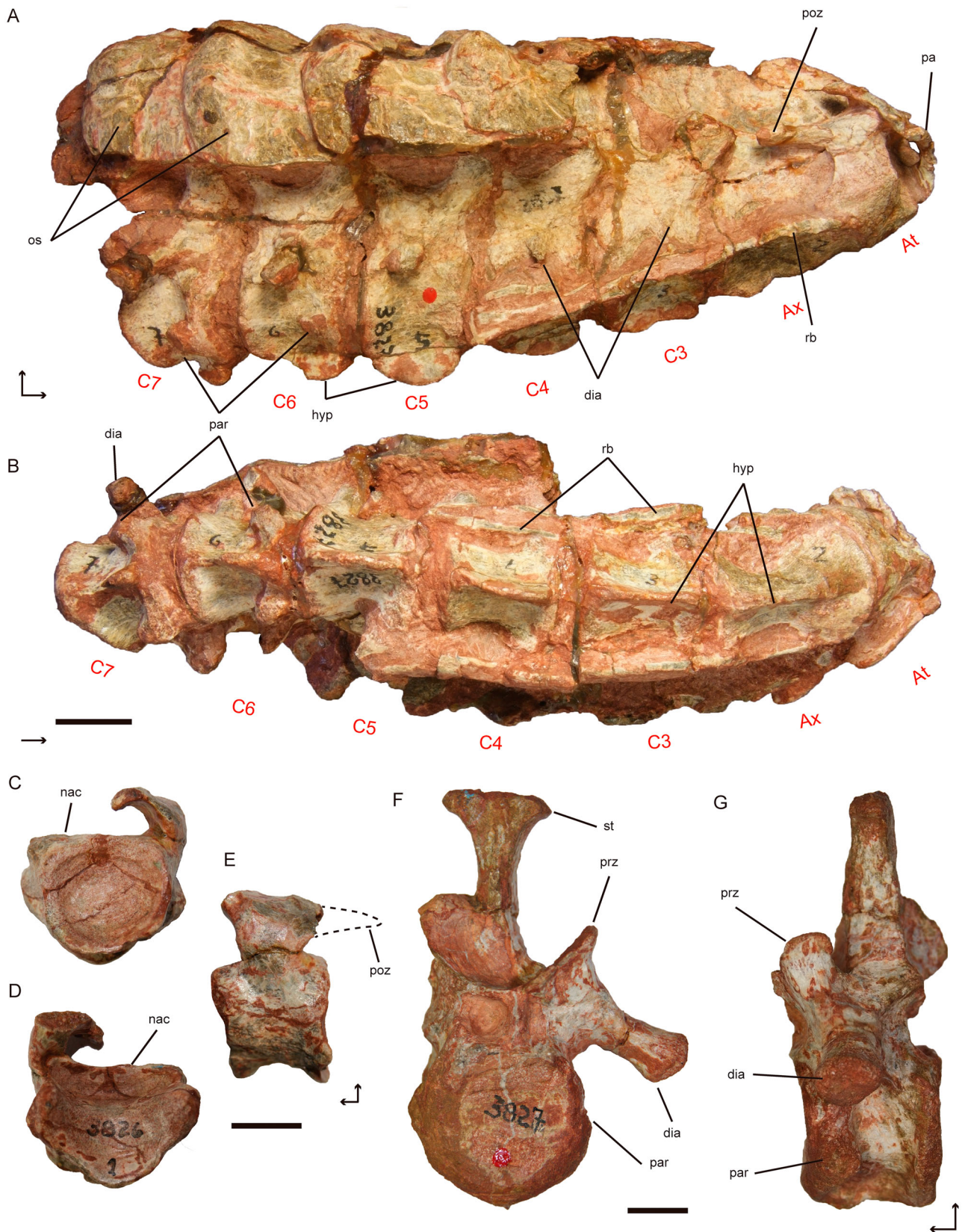
FIGURE 3. Cervical vertebrae of *Riojasuchus tenuisceps*. Articulated cervical vertebrae 1–7 of PVL 3827 in **A**, lateral and **B**, ventral views; atlas of PVL 3826 in **C**, anterior, **D**, posterior, and **E**, lateral views; cervical vertebra 8 of PVL 3827 in **F**, anterior and **G**, lateral views. Arrows indicate dorsal and anterior directions. **Abbreviations**: **dia**, diapophysis; **hyp**, hypapophysis; **nac**, neural arch contact; **os**, osteoderm; **pa**, proatlas; **par**, parapophysis; **poz**, postzygapophysis; **prz**, prezygapophysis; **rb**, rib; **st**, spine table. Scale bars equal 20 mm (**A–B**) and 10 mm (**C–G**).
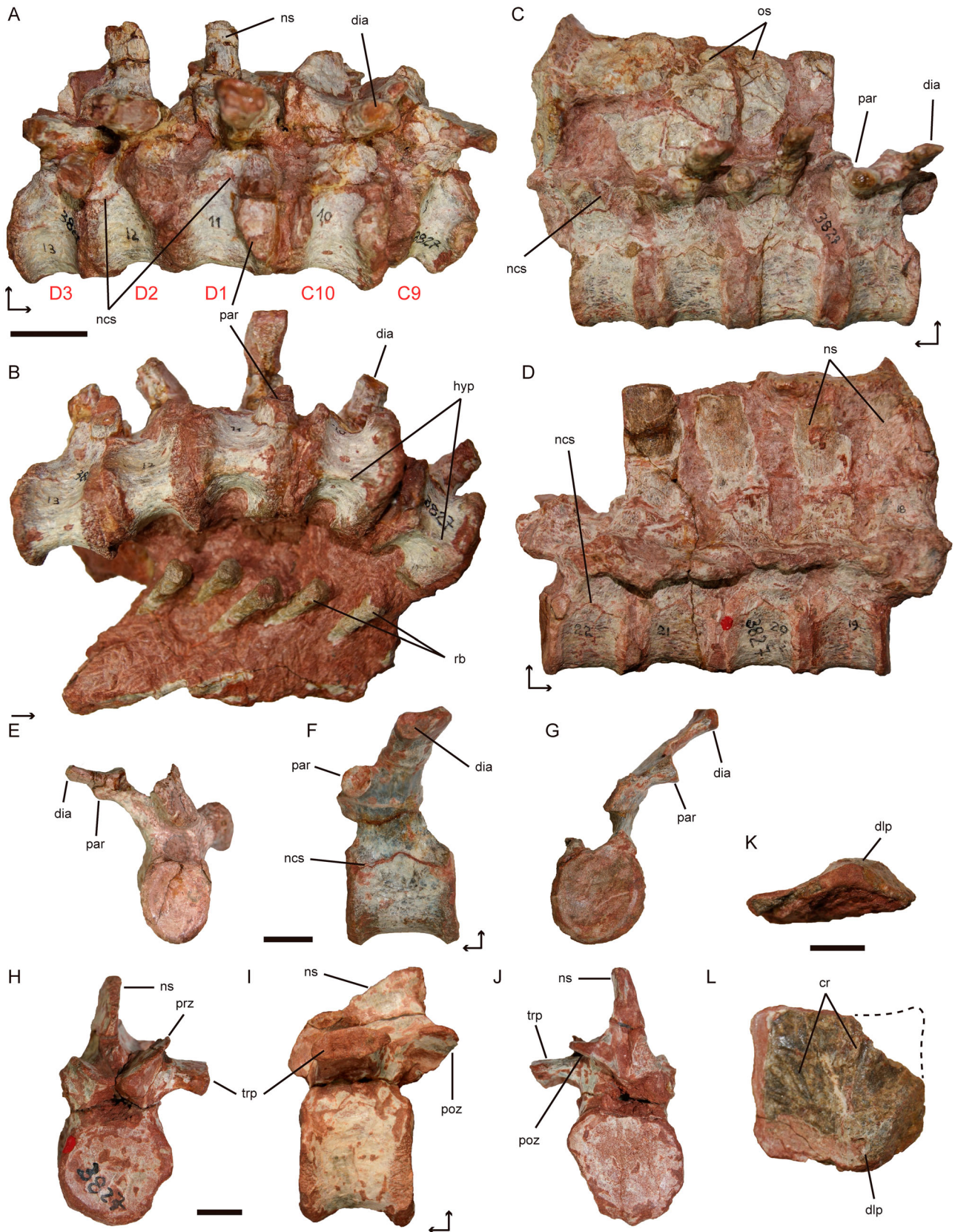
FIGURE 4. Posterior cervical vertebrae and dorsal vertebrae of *Riojasuchus tenuisceps*. Articulated presacral vertebrae 9–13 of PVL 3827 in **A**, lateral and **B**, ventral views; articulated mid-dorsal vertebrae of PVL 3827 in **C**, left lateral, **D**, right lateral, and **E**, posterior views; posterior dorsal vertebra of PVL 3828 in **F**, lateral and **G**, anterior views; last dorsal vertebra of PVL 3827 in **H**, anterior, **I**, lateral, and **J**, posterior views; isolated dorsal osteoderm of PVL 3814 in **K**, anterior and **L**, dorsal views. Arrows indicate dorsal and anterior directions. **Abbreviations**: **cr**, crest; **dia**, diapophysis; **dlp**, dorso-lateral prominence; **hyp**, hypapophysis; **ncs**, neurocentral suture; **ns**, neural spine; **os**, osteoderm; **par**, parapophysis; **poz**, postzygapophysis; **prz**, prezy-gapophysis; **trp**, transverse process. Scale bars equal 20 mm (**A–D**) and 10 mm (**E–L**).

was identified as four dorsal vertebrae of the middle to posterior region of the dorsal series (Fig. 4A–D). The referred specimen, PVL 3828, has 10 dorsal vertebrae preserved, but most of these are only represented by their centrum excepting one, a posterior dorsal vertebra, which has its left diapophysis and parapophysis well preserved.

The anterior dorsal vertebrae of *Riojasuchus tenuisceps* (PVL 3827) resemble the general shape of the preceding cervical vertebrae and has the parapophyses located above the dorsoventral midline of the centrum as well. However, the anterior dorsal vertebrae differ from the cervical vertebrae because the base of the parapophyses of the first dorsal vertebra (D1) expands dorsally, contacting the neurocentral suture (Fig. 4A). Moreover, D1 lacks a hypapophysis and the ventral surface of its centrum is flat, unlike the anteroposteriorly concave centrum of the succeeding dorsal vertebrae (Fig. 4B).

In general terms, the anterior dorsal vertebrae (PVL 3827: D1–D3; Bonaparte, 1972: 'dorsals 11–13') are slightly shorter than tall and they are barely laterally compressed (Fig. 4A, B). The anterior and posterior articular facets are almost circular and slightly concave. The lateral surfaces of the centrum are markedly anteroposteriorly concave and lack lateral fossae. No accessory laminae could be recognized between the apophyses or between the centrum and the apophyses. The ventral surface of the centrum is gently concave and does not have a hypapophysis as in the cervical vertebrae. The diapophyses are located dorsal to the neurocentral suture; they are long and posterolaterally projected (Fig. 4A, B). The posterolateral direction of the diapophyses is not as posteriorly inclined as that observed in middle dorsal vertebrae. The parapophyses of the first anterior dorsal vertebrae (D1) are located in the middle region of the anterior margin of the centrum, although toward the third dorsal vertebrae (D3) the parapophyses are located on the anterodorsal margin of the centrum (Fig. 4A). The parapophyses of the anterior dorsal vertebrae contact the neurocentral suture and are located ventral to the diapophyses; they are short and laterally projected. The neural spines of the anterior dorsal vertebrae are anteroposteriorly short and dorsoventrally oriented. They are taller than the centra, but their total height could not be determined because all the preserved spines are missing their apical region; therefore, it is also unknown whether they expanded into a spine table as seen in the cervical vertebrae or not (Fig. 4A). Pre- and postzygapophyses are too damaged to allow the observation of any detail in both specimens PVL 3827 and PVL 3828. The ribs corresponding to the anterior dorsal vertebrae were preserved near their natural position (Fig. 4B). These bicipit ribs are partially articulated and still covered by sediment; they are posteroventrally curved, and the capitulum is disarticulated and exposes an oval-shaped articular surface. The tuberculum of these ribs is not exposed.

The middle region of the dorsal series is represented by an articulated series of four centra plus a fifth neural spine of PVL 3827 and several disarticulated centra of PVL 3828. The centrum of the middle dorsal vertebrae is approximately as long as high and laterally compressed. The anterior and posterior articular facets are oval, being higher than wide and gently concave. The lateral and ventral surfaces of the centrum are anteroposteriorly concave and lack of lateral fossae and hypapophysis (PVL 3827, PVL 3828). The diapophyses are located at the level of the postzygapophyses; they are elongated and project posterolaterally with a marked dorsal orientation as well. They are located immediately posterodorsal to the parapophyses and at the anteroposterior midline of the centrum (Fig. 4C–E). The parapophyses are located on the lateral margin of the anterior articular facet of the centrum; its base is fused to the base of the diapophyses, and it projects laterally just anteroventral to the latter. The parapophyses are therefore located dorsal to the neurocentral suture and elevated at a height equivalent to

the height of the centrum. The neural spines of the middle dorsal vertebrae are high, being 1.5 times higher than the centrum (Fig. 4C, D); they are anteroposteriorly longer than the neural spines of the anterior dorsal vertebrae and do not expand toward their apex, differing from the spine tables of the cervical region. The neural spines of these dorsal vertebrae are posterodorsally oriented at ca. 10° from the vertical plane. The prezygapophyses and postzygapophyses were preserved in articulation, and their articular facet cannot be observed. The prezygapophyses extend slightly anterior to the anterior margin of the centrum, whereas the postzygapophyses are almost entirely projected posterior to the posterior margin of the centrum.

The posterior dorsal vertebrae of *R. tenuisceps* are represented by a fairly complete vertebra, previously identified by Bonaparte (1972) as adjacent to the middle dorsal section of the holotype (PVL 3827: 'dorsal 24'), and by several disarticulated/isolated centra of the specimen PVL 3828, from which only one has preserved the complete left apophyses (Fig. 4F–J). These vertebrae are almost equally high as wide, with anterior and posterior articular facets concave and circular. The parapophyses and diapophyses are fused together on their bases, but their articular surfaces are still differentiated (Fig. 4F, G) and they fuse completely into transverse processes toward the last dorsal vertebrae (Fig. 4H–J). The parapophyses are located at the level of the anterior margin of the centrum; they are short, circular in section, and dorsolaterally directed with a slight anterior orientation. The diapophyses are located at the anteroposterior midline of the centrum; they are almost three times longer than the parapophyses, oval in section, and project dorsolaterally. On the posterior-most vertebrae, the transverse processes are anteroposteriorly wide and project laterally. The prezygapophyses, postzygapophyses, and neural spine were only preserved on the isolated vertebra of PVL 3827 (Fig. 4H–J). The prezygapophyses have oval articular facets that are oriented at 40° from the horizontal plane, and the postzygapophyses have more rounded facets and are oriented at 30° from the horizontal plane. Only the base of a neural spine was preserved; it is anteroposteriorly longer than that of the middle dorsal vertebrae, but its orientation cannot be determined. No accessory fossae, laminae, or hypapophysis could be identified on these posterior dorsal vertebrae.

Sacral Vertebrae—There are three sacral vertebrae in *R. tenuisceps*; these were preserved in articulation in the holotype (PVL 3827) and partially disarticulated in the referred specimen PVL 3828. The centrum of the sacral vertebrae is more robust than that of the cervical and dorsal vertebrae, being wider than high and equally wide as long. The centrum has no hypapophysis on its ventral surface, as the previous dorsal vertebrae, and no fossae or accessory laminae on its lateral surface. The anterior and posterior articular surfaces are almost flat and suboval in shape. The base of the laterally projecting transverse processes is almost circular in section (Fig. 5A, B), which contrasts with the dorsoventrally flat base of the transverse processes of the posterior dorsal vertebrae. The transverse processes of the sacral vertebrae are short and robust and would articulate with the medial surface of the ilium. The transverse processes of the second sacral are twice as wide as those of the first sacral. The neural spines of the first and second sacral vertebrae of the holotype (PVL 3827) were preserved but seem to be fused to each other (Fig. 5A). These spines are 1.5 times higher than the centrum; they do not expand on its distal tips, neither laterally nor anteroposteriorly (Fig. 5A). The fusion of the sacral spines, as well as that of the corresponding centra, appears to be a pathology in PVL 3827 because the centra of all the sacral vertebrae of the referred specimen of the same-size PVL 3828 are disarticulated, which implies that in a normal condition the sacral vertebrae of PVL 3827 should not have been fused to each other.

Caudal Vertebrae—The caudal vertebrae of *R. tenuisceps* are shorter than the sacral vertebrae, and their centra are spool-
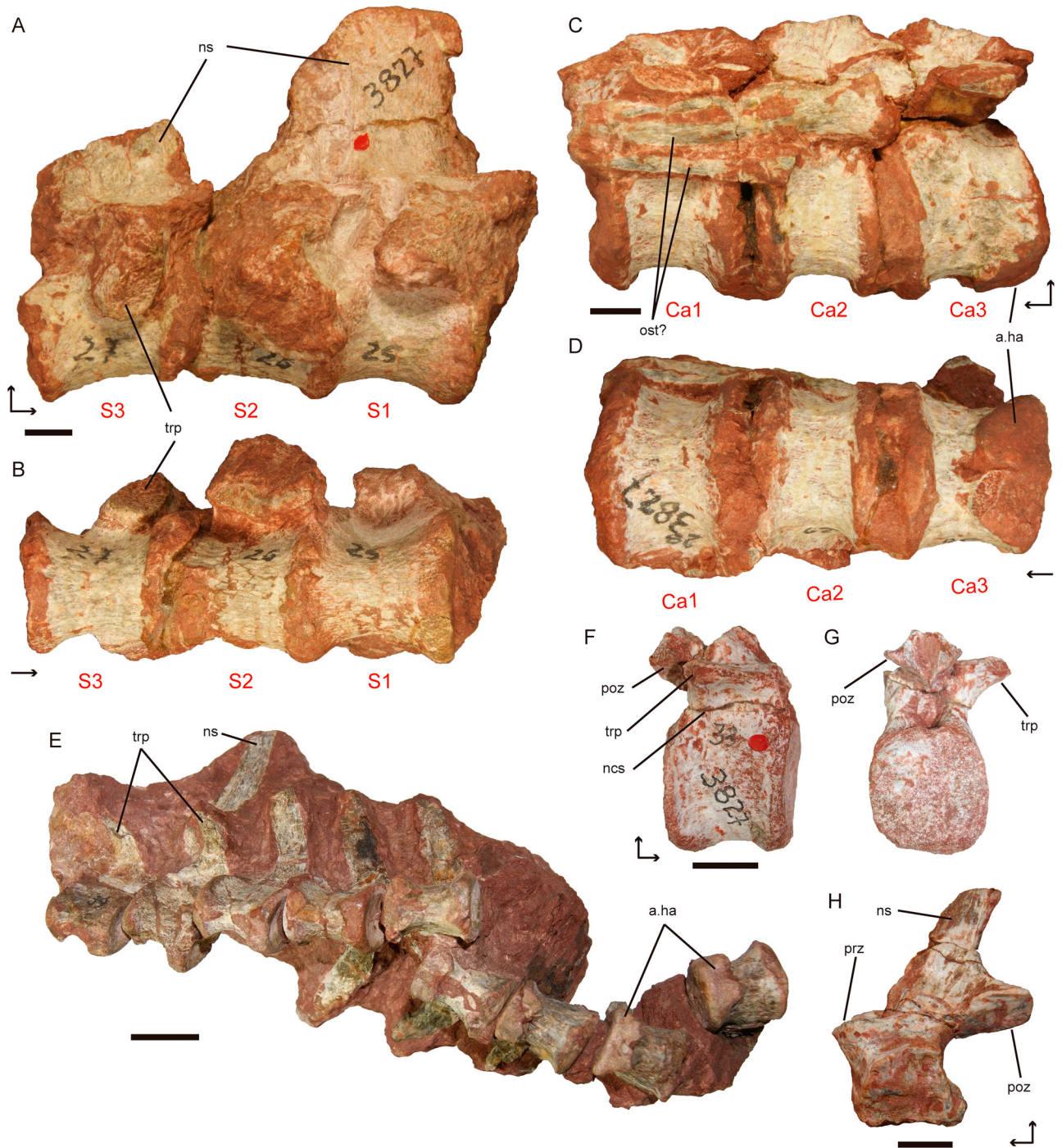
FIGURE 5. Sacral and caudal vertebrae of *Riojasuchus tenuisceps*. Articulated sacral vertebrae of PVL 3827 in **A**, lateral and **B**, ventral views; first three caudal vertebrae of PVL 3827 in **C**, lateral and **D**, ventral views; **E**, nine caudal vertebrae of PVL3828 in ventrolateral view; isolated caudal vertebra of PVL 3827 in **F**, lateral and **G**, posterior view; **H**, isolated caudal neural arch of PVL 3826 in lateral view. Arrows indicate dorsal and anterior directions. **Abbreviations**: **a.ha**, articulation for the hemal arches; **ncs**, neurocentral suture; **ns**, neural spine; **ost?**, possible ossified tendons; **poz**, postzygapophysis; **prz**, prezygapophysis; **trp**, tranverse process. Scale bars equal 10 mm.

shaped. The anterior caudal vertebrae are almost as high as wide, with the middle to posterior ones laterally compressed and more elongated (PVL 3827, PVL 3828; Fig. 5F, G, I, J). The anterior articular facet of the caudal vertebrae is slightly concave, whereas the posterior one is flat (PVL 3828). On the posterior margin of the ventral surface of the centrum, two articular facets for the hemal arches can be recognized. These facets are oval, anteroposteriorly elongated, on the anterior caudal vertebrae and more rounded toward the posterior ones (PVL 3828; Fig. 5D, E). The first two caudal vertebrae had no hemal

arches because they do not have the corresponding articular facets (PVL 3827, PVL 3828; Fig. 5D). The lateral surfaces of the caudal centra lack both lateral fossae and accessory laminae between the centrum and the apophyses (Fig. 5E–H). The transverse processes are elongated, posterolaterally directed, and located dorsal to the neurocentral suture (Fig. 5E–G). The prezygapophyses barely extend beyond the anterior margin of the centrum; their articular facets are oval, concave, and dorsomedially oriented at 40° from the horizontal. The postzygapophyses are more elevated and extend almost entirely posterior to the posterior margin of the centrum; the articular facets are flat to slightly concave, ventromedially directed at 45° from the horizontal, a more pronounced angle than that of the posterior dorsal vertebrae (Fig. 5F–H). Neural spines are anteroposteriorly short and posterodorsally directed at 25° from the vertical axis. Even though their surface has been damaged during their original preparation, it is evident that the caudal neural spines keep the same width along their entire length and that they do not expand laterally on their distal ends, as described in the previous dorsal and sacral series (PVL 3826, PVL 3828) (Fig. 5E–H).

The first caudal vertebrae of PVL 3827 have some anteroposteriorly oriented rod-like ossifications on the left side of the centra. These are slightly laterally compressed, are located ventral to the transverse processes, and could possibly be interpreted as ossified tendons (Fig. 5F). This condition seen in *Riojasuchus* is quite uncommon because the ossified tendons preserved in other archosaurs are located in the epiaxial region, dorsal to the transverse processes and lateral to the neural spines (e.g., sauropods, hadrosaurs, ankylosaurs) (Forster, 1990; Coombs, 1995; Organ, 2006; Cerda et al., 2015b).

Ribs—Few cervical and dorsal ribs were preserved in *Riojasuchus tenuisceps*. The anterior-most cervical ribs were preserved articulated from the first to the fourth cervical vertebra of PVL 3827, but they were overprepared and are currently reduced to anteroposteriorly oriented thin bone rods attached to the ventrolateral margins of the centra (Fig. 3A, B). On the other hand, the ribs corresponding to the last two cervicals and first three dorsals were preserved in better condition but still partially covered by sediment. These ribs are slightly detached from their corresponding articular surfaces on the vertebrae (Fig. 4B). They are posteroventrally curved and have a well-differentiated tubercule, although the capitulum is still covered by sediment in all the preserved ribs. No gastralia are preserved in any specimen of *R. tenuisceps*.

Osteoderm Morphology and Histology

External Morphology—*Riojasuchus tenuisceps* has only one paired line of paramedian osteoderms arranged in a one-on-one relationship with the vertebrae. Cervical osteoderms are rectangular in shape, being twice wider than long, and have a marked rounded prominence on their posterolateral corner (Fig. 3A). The external surface of the cervical osteoderms of PVL 3827 has been overprepared and therefore lacks any kind of ornamentation, but some isolated osteoderms of PVL 3814 have a smooth ornamentation with radial low crests and short deep grooves. Four dorsal osteoderms of PVL 3827 were preserved displaced from their natural position, covering the left side of the neural spines of the middle dorsal vertebrae, and several osteoderms associated with PVL 3814 were preserved disarticulated (Fig. 4C, K, L). These are subquadrangular, with their anterior margin slightly convex and the posterior one concave. The dorsal osteoderms have the same kind of ornamentation of short radial crests and grooves seen in the cervical region, although the dorsolateral prominence is more strongly developed (Fig. 4C, K, L). No articular surfaces could be recognized on the preserved osteoderms; however, they articulate dorsally, overlapping the anterior margin of the subsequent osteoderm. There are

no sacral or caudal osteoderms preserved in any of the four specimens of *Riojasuchus tenuisceps* (PVL 3827, PVL 3828, PVL 3826, PVL 3814).

Histological Description—The sectioned elements of PVL 3814 are wider than thick (ca. 1/9) and have a trilaminar structure, in which two distinct cortices (external and basal) of compact bone can be differentiated from an internal core of cancellous bone. The basal surface texture is flat and strongly convex in transverse section. The external cortex has been eroded in several areas. Nevertheless, a smooth ornamentation in the external surface, which consists of low ridges (convex surface) and short deep grooves (concave surface), is still preserved in some areas of the samples (Fig. 6A, B).

The basal cortex is thin (ca. 300 μm), and it is mainly formed by secondary bone tissue. The cortical bone is almost avascular, showing few longitudinal canals. Some circumferentially oriented isolated simple canals and some primary osteons are present as well. The preserved portions of primary matrix are composed of parallel-fibered bone (Fig. 6C–D). Three lines of arrested growth (LAGs) are counted in the basal cortex (Fig. 6E).

The cancellous bone occupies most of the osteoderm in section. This is composed of long and thin trabeculae formed by secondarily deposited lamellar bone tissue, which is evidenced by cementing lines. Intertrabecular spaces are considerably large in one of the sampled osteoderms (Fig. 6F–H).

Whereas the thickness of the external cortex is roughly equal to that of the basal cortex in the dorsal osteoderm (Fig. 6A), a different condition is recognized in the cervical osteoderm (section R 2b), in which this cortex is at least 2–3 times thicker than the basal one (Fig. 6B). In general, the main composition of the external cortex is remodeled bone tissue. Preserved remains of primary bone are composed of parallel-fibered tissue. Because of the low grade of preservation and missing portions of the element during sectioning, it is not possible to infer the mechanism of formation of external surface ornamentation. The cortical bone is poorly vascularized, with longitudinal and circumferential canals (Fig. 6I–K). A variation to this pattern is observed in the cervical osteoderm sample (section R 2b), which is highly vascularized, with secondary canals oriented parallel to the section plane (Fig. 6K). There is no evidence of the presence of Sharpey's fibers in the whole thickness of the osteoderms.

Appendicular Skeleton

The scapular girdle is formed by the articulated scapula and coracoid and has been preserved, partially at least, in three specimens of *Riojasuchus tenuisceps* (PVL 3826, PVL 3827, PVL 3828).

Scapula—The scapula is tightly sutured to the coracoid (Fig. 7A–C) and has a wide ventral end that narrows abruptly toward the base of the scapular blade (PVL 3827, PVL 3828). The scapular blade is oval in cross-section, being twice wider anteroposteriorly than thick lateromedially. The dorsal margin of the scapular blade is slightly convex; its anterior margin is straight, and its posterior margin is markedly convex (Fig. 7E). Toward the dorsal end, the anterior margin is gradually expanded anteriorly whereas the posterior margin expands abruptly. Because of this expansion, the dorsal end of the scapula is almost twice as wide as the scapular neck, which can also be seen in several archosauriforms (e.g., *Erythrosuchus africanus*: Gower, 2003; *Nicrosaurus kapffi*: SMNS 6328; *Euparkeria capensis*: cast SAM-PK 5867; *Parringtonia gracilis*: NHMUK PV R8646; *Ticinosuchus ferox*: Lautenschlager and Desojo, 2011; *Caiman yacare*: MACN-He 48841; *Lewisuchus admixtus*: PULR 01). The acromial process can be recognized in the ventral region of the scapula; it is well developed, projecting toward the lateral surface (Fig. 7A, D). The scapula forms the dorsal third of the glenoid fossa, which is delimited by a well-developed
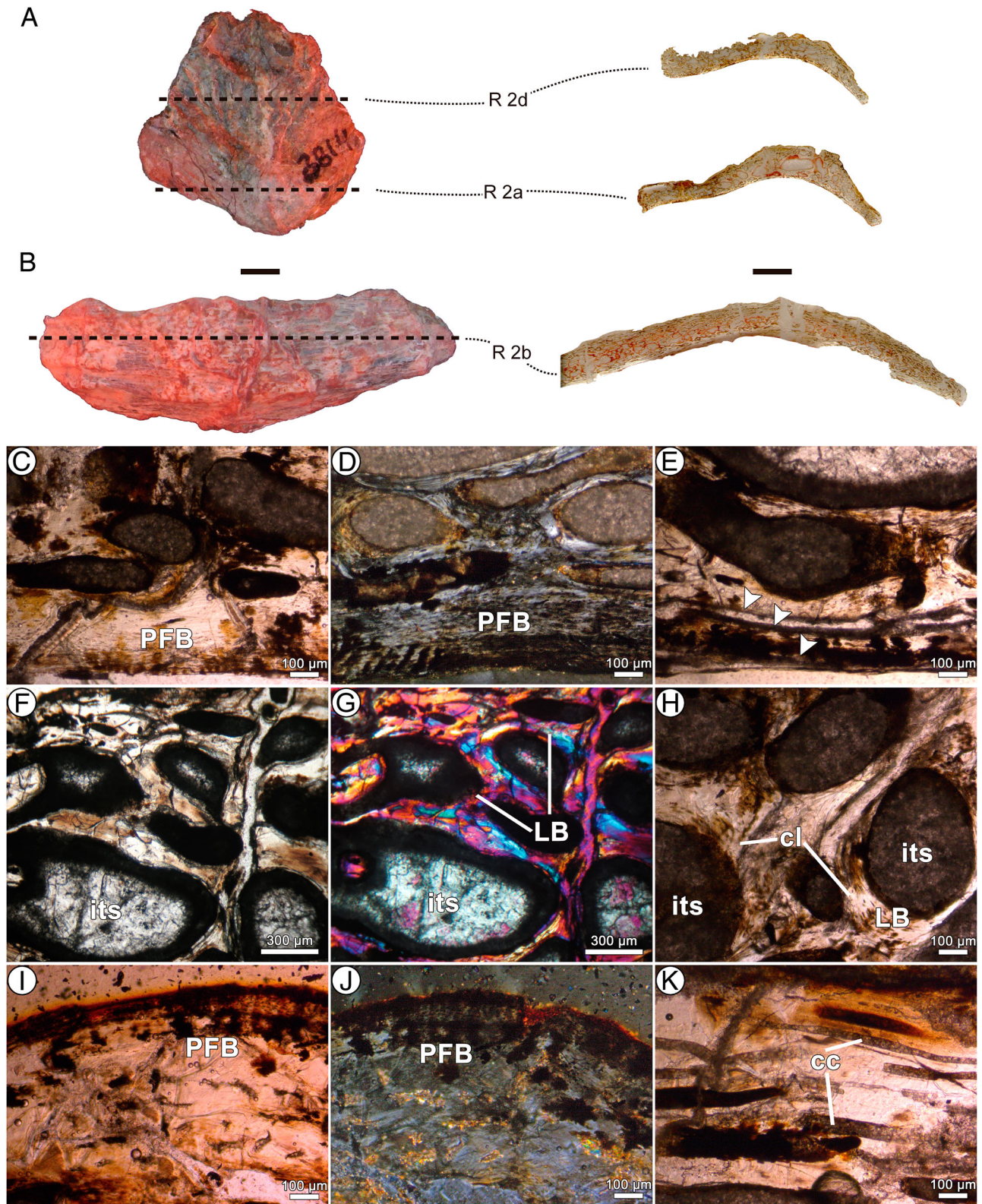
FIGURE 6. *Riojasuchus tenuisceps*, histology of osteoderms of PVL 3814. External view of **A**, dorsal osteoderm and its transverse sections (R 2d, R 2a) and **B**, cervical osteoderms and its transverse section (R 2b); **C**, **D**, detail of the basal cortex; **E**, basal cortex showing three LAGs; **F**, **G**, detail of cancellous bone of internal region; **H**, close up to internal region; **I–J**, detail of external cortex (ridge of ornamentation); **K**, detail of external cortex of R 2b section. **C**, **E–F**, **H–I**, **K**, under normal light; **D**, **J**, under cross-polarized light; **G**, under cross-polarized light with lambda compensator. **Abbreviations**: **cc**, circumferential canal; **cl**, cementing line; **its**, intetrabecular space; **LB**, lamellar bone; **PFB**, parallel-fibered bone. Scale bars equal 50 mm (**A**, **B**).
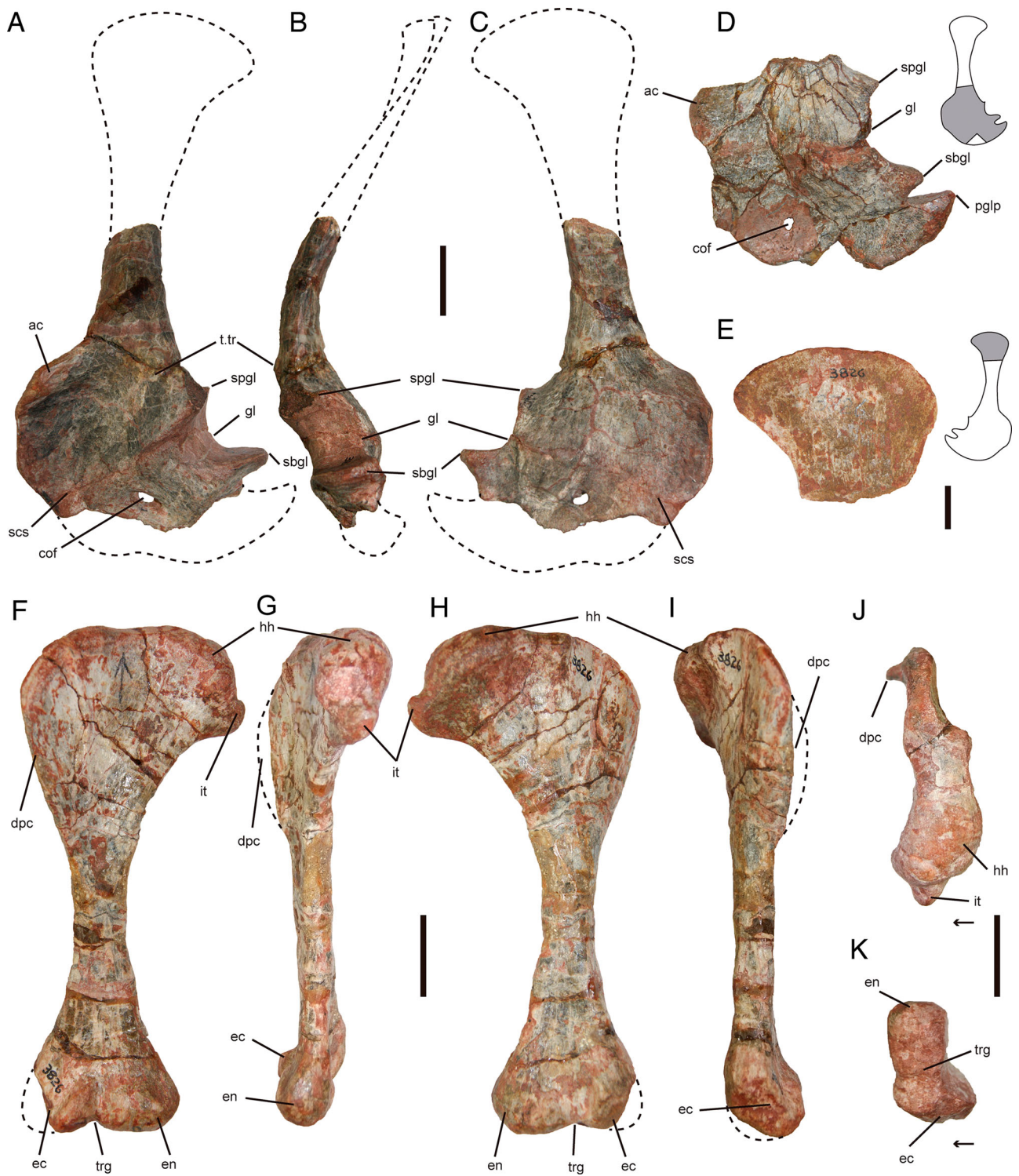
FIGURE 7. Pectoral girdle and humerus of *Riojasuchus tenuisceps*. Fragmentary left scapula and coracoid of PVL 3827 in **A**, lateral, **B**, anterior, and **C**, medial views; **D**, fragmentary left scapula and coracoid of PVL 3828 in lateral view; **E**, distal end of scapular blade of PVL 3826. Arrows indicate anterior direction. **Abbreviations**: **ac**, acromion; **cof**, coracoid foramen; **dpc**, deltopectoral crest; **ec**, ectepicondyle; **en**, entepicondyle; **gl**, glenoid fossa; **hh**, humerus head; **it**, internal tuberosity; **pglp**, postglenoid process; **sbgl**, subglenoid lip; **scs**, scapulocoracoid suture; **spgl**, supraglenoid lip; **t.tr**, tubercule for the M. triceps; **trg**, trochlear groove. Scale bars equal 20 mm (**A–D**, **F–I**) and 10 mm (**E**, **J–K**).

supraglenoid rim that is shorter than the subglenoid lip of the coracoid (Fig. 7A–D). The dorsolateral surface of the ventral end of the scapula has an oval tuberosity that could be associated with the insertion of the M. triceps (Fig. 7A), resembling that seen in the loricatans *Batrachotomus kupferzellensis* (SMNS 80271) and *Prestosuchus chiniquensis* (SNSB-BSPG AS XXV 12), but

differing from this element of most arcosauriforms, in which this tuberosity is much smaller (Nesbitt, 2011:char. 219).

Coracoid—The coracoid of *R. tenuisceps* is semicircular, being rounded on its anterior margin. It forms the lower two-thirds of the glenoid fossa, which is posteroventrally oriented and has a marked subglenoid rim projecting posteriorly further than the supraglenoid rim of the scapula (Fig. 7A–C). The subglenoid rim is separated from the postglenoid process by a deep furrow. The postglenoid process is short but extends slightly posterior to the subglenoid rim (Fig. 7D), as also happens in *Ornithosuchus woodwardi* (NHMUK PV R3916), rauisuchians (e.g., *Batrachotomus kupfezellensis*: SMNS 80271; *Postosuchus kirkpatricki*: TTU-P09002; *Prestosuchus chiniquensis*: BSPG AS XXV 12), and dinosauriforms (e.g., *Lewisuchus admixtus*: PULR 01). The posteroventral margin of the coracoid is smooth in PVL 3828, and no furrow or notch could be recognized for the articulation of the clavicle as those seen in crocodilomorphs or the loricatan *Postosuchus kirkpatricki* (Weinbaum, 2013; TTU-P09002). The coracoid foramen for the passage of the supracoracoid nerve is located anterior to the glenoid fossa; it is circular and surrounded by a well-delimited oval fossa on the lateral surface of the coracoid (PVL 3827, PVL 3828) (Fig. 7A, D). This fossa is absent on most archosauriforms and was only recognized on the loricatans *Batrachotomus kupferzellensis* (SMNS 80271) and *Prestosuchus chiniquensis* (SNSB-BSPG AS XXV 2).

Humerus—The humerus of *Riojasuchus tenuisceps* is slender and slightly sigmoid in medial view. The proximal end is remarkably expanded in a fan shape, being four times wider than the shaft and twice wider than its distal end (Fig. 7F–I). The head of the humerus is globose and has a medially projected internal tuberosity (PVL 3827, PVL 3826) (Fig. 7F–J). The head is restricted to the anterior half of the proximal surface of the humerus in *Riojasuchus tenuisceps* (PVL 3827, PVL 3826) as in most archosaurs. The deltopectoral crest extends along the proximal third of the humerus of *Riojasuchus tenuisceps* and projects anteriorly from the lateral margin; it is moderately developed and forms a 90° angle with the sagittal plane (PVL 3827) (Fig. 7F–J). The shaft of the humerus is slightly twisted, and as a result the main axis of the proximal end is rotated 25° from that of the distal end. The cross-section of the shaft is elliptic, being twice lateromedially wider than anteroposteriorly thick. The distal end of the humerus is ca. 2.5 times wider than the shaft and has well-developed ent- and ectepicondyles (Fig. 7K). The ectepicondyle is posteriorly expanded, almost duplicating the anteroposterior thickness of the entepicondyle, and it is slightly lateromedially shorter than the latter, from which it is separated by a shallow trochlear groove (Fig. 7F, H, K). The humerus has no ectepicondylar groove on its lateral surface. The ectepicondyle of *R. tenuisceps* (PVL 3826, PVL 3827, PVL 3828) also lacks an entepicondylar foramen as that seen in aetosaurs (e.g., *Neoaetosauroides engaeus*: PVL 3525; *Desmatosuchus smalli*: Parker, 2005) or a lateral supinator process as that of loricatans (e.g., *Postosuchus kirkpatricki*: TTU-P09000; *Batrachotomus kupferzellensis*: SMNS 80276).

Radius—The radius of *R. tenuisceps* is known by the proximal end and the distal half of PVL 3828, and the distal half preserved in articulation with the carpus in PVL 3827 (Fig. 8A–G). The radius is an elongate element with an expanded proximal end that abruptly triplicates the width of the shaft. The proximal surface is concave and triangular, with a slight globous projection on its medial margin for its articulation with the humerus (Fig. 8D, E). The distal end of the radius becomes anteroposteriorly expanded and mediolaterally flattened, resulting in an oval cross-section with its main axis anteroposteriorly oriented (PVL 3827, PVL 3828) (Fig. 8A–C). The medial surface of the distal end of the radius is flat, whereas the lateral surface is slightly concave. The complete distal surface of the radius articulates with the radiale but does not contact the intermedium (PVL 3827) (Fig. 8F, G).

Ulna—The ulna of *R. tenuisceps* is a gracile, slightly sigmoid element that is barely 10% shorter than the humerus. The proximal end of the ulna is triangular in cross-section and has a well-developed olecranon with a well-defined articular surface for the humerus (PVL 3828) (Fig. 8A–C). This articular surface is concave and is anteriorly delimited by a crest that separates it from the contact surface for the radius (Fig. 8A–C). The lateral surface of the proximal half of the ulna is convex, whereas the medial surface is concave. The shaft is 2.5 times narrower than the proximal end; it curves anteriorly and is subcircular in cross-section. The distal end of the ulna is laterally compressed, and its main axis is perpendicular to that of the proximal end. Two articular facets can be recognized on the distal margin of the ulna, the lateral one for the ulnare and the medial one for the intermedium (PVL 3827) (Fig. 8A–C).

Carpus—It has been exceptionally well preserved in full articulation in the holotype of *R. tenuisceps* (PVL 3827). The proximal carpals are proximodistally short as in most archosauriforms. The radiale is an almost cubic element, more robust than the ulnare, with a concave proximal surface for the articulation of the radius, a slightly concave lateral surface for the articulation of the intermedium, and a convex distal surface that contacts the metacarpal I (Fig. 8F–J). The dorsal surface of the radiale has a deep concavity on its proximolateral corner, restricted by a thick oblique crest that extends proximomedially. The medial surface of the radiale is slightly concave, and the distal surface has a marked thickening on its proximal half. The intermedium is a dorsoventrally flattened element that articulates medially with the radiale, laterally with the ulnare and the ulna, and distally with the metacarpals II and probably III. The intermedium is pentagonal in dorsal view and slightly longer than the radiale (Fig. 8F, G). Its dorsal surface is flat, whereas its ventral surface is concave. The ulnare is quadrangular in dorsal view, slightly laterally thinner than proximodistally long, and it is dorsoventrally depressed (Fig. 8F, G). It is slightly narrower than the radiale and the intermedium, and its dorsal and ventral surfaces are concave. The proximal carpals configuration of *Riojasuchus tenuisceps* differs from that of basal crocodylomorphs, which have a pisciform carpal located lateral to the ulnare and lack an intermedium carpal (e.g., *Protosuchus richardsoni*: Colbert and Mook, 1951; *Hesperosuchus agilis*: Colbert, 1952).

Metacarpals—The metacarpals of *R. tenuisceps* were partially preserved in the holotype, in articulation with each other specimen, and they are slightly offset from the carpus. The metacarpal I is the only element completely preserved, whereas the metacarpals II to V lost their distal ends (Fig. 8F, G). The proximal end of the metacarpal I is markedly dorsoventrally expanded, triplicating the thickness of the shaft, but the distal end is barely expanded compared with the shaft. On the other hand, the lateromedial expansion of both ends of the metacarpal I is very slight. The condyles of the proximal end are offset from the horizontal plane, with the lateral condyle being more dorsally located than the medial one. The condyles of the distal end of the metacarpal I are asymmetric, with the lateral one being more expanded than the medial one. It is not possible to identify with certainty whether the distal end has an articular ginglymus because it is partially covered by sediment. Both lateral surfaces of the distal end of the metacarpal have a fossa (Fig. 8F). The preserved region of the metacarpals II to V corresponds to the proximal end and shaft. Their proximal ends are lateromedially expanded but do not duplicate the width of the shafts, and the medial corners of the metacarpals dorsally overlap the lateral corner of the adjacent one. The proximal articular surfaces are covered by sediment excepting that of metacarpal IV, which is barely concave.

Manual Phalanges—Only two manual phalanges of *Riojasuchus tenuisceps* were preserved (PVL 3827): the first phalanx from digit I and a disarticulated one that is misplaced between
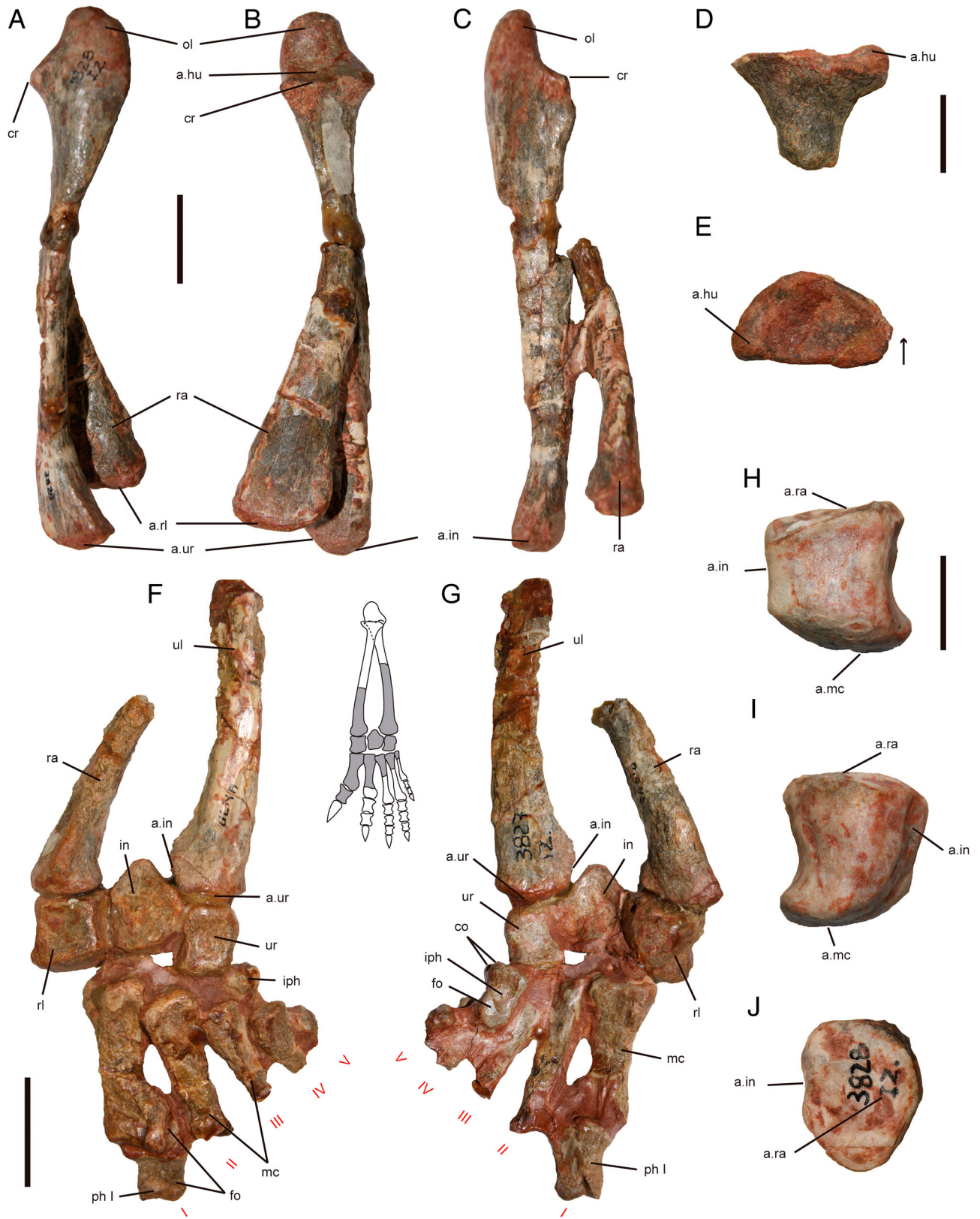
FIGURE 8. Radius, ulna and manus of *Riojasuchus tenuisceps*. Articulated lef ulna and partial radius of PVL 3828 in **A**, lateral, **B**, anterior, and **C**, medial views; isolated proximal end of radius of PVL 3828 in **D**, lateral and **E**, proximal views; incomplete articulated radius, ulna, and manus of PVL 3827 in **F**, anterior and **G**, posterior views; isolated right radiale in **H**, dorsal, **I**, ventral, and **J**, proximal views. Arrows indicate anterior direction. **Abbreviations**: **a.hu**, articulation for the humerus; **a.in**, articulation for the intermedium; **a.mc**, articulation for the metacarpals; **a.ra**, articulation for the radius; **a.rl**, articulation for the radiale; **a.ur**, articulation for the ulnare; **fo**, fossa; **iph**, isolated phalanx; **ol**, olecranon; **ph I**, phalanx I-1; **ra**, radius; **rl**, radiale; **ul**, ulna; **ur**, ulnare. Scale bars equal 20 mm (**A–C**, **F**, **G**) and 10 mm (**D**, **E**, **H–J**).
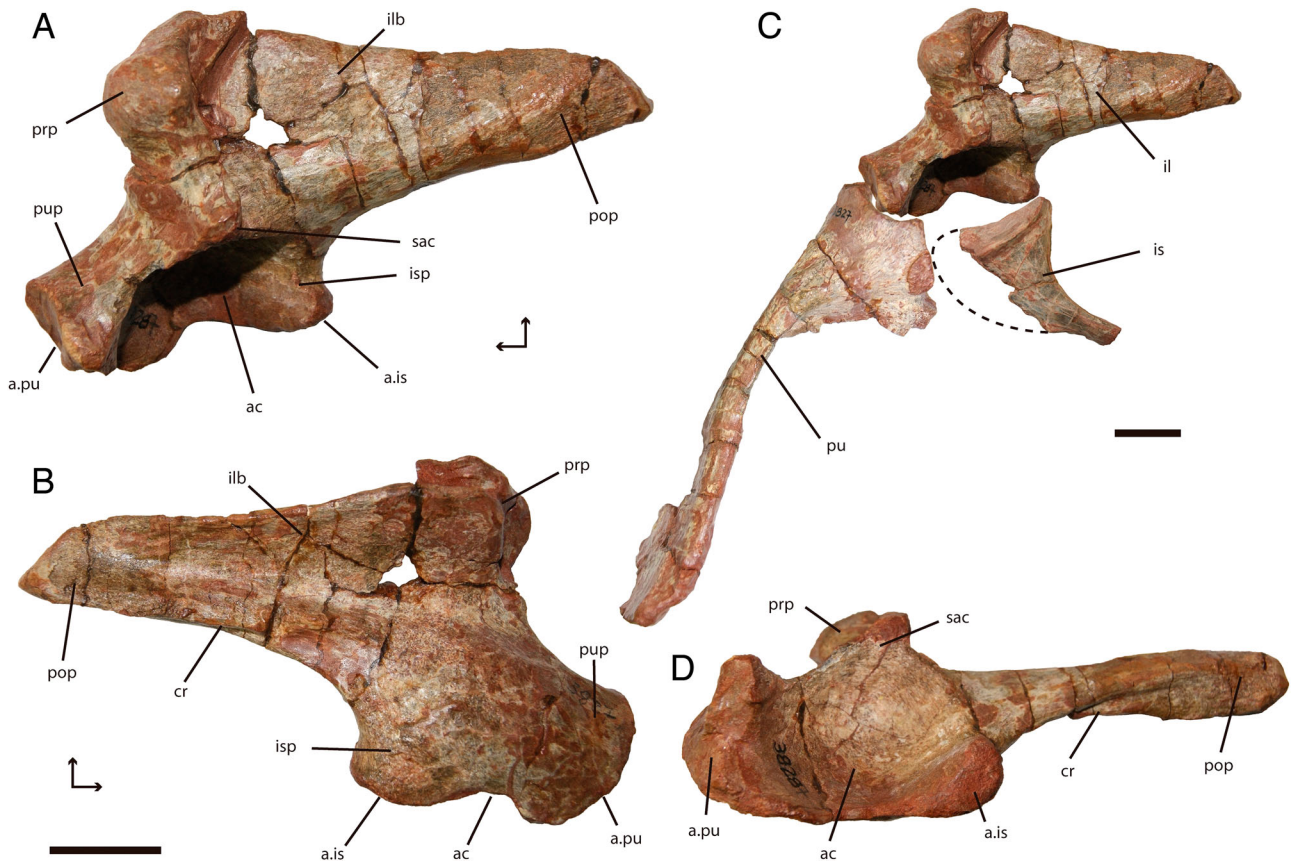
FIGURE 9. Pelvic elements of *Riojasuchus tenuisceps*. Left ilium in **A**, lateral and **B**, medial views; **C**, left ilium, pubis, and ischium (mirrored) in articulation in lateral view; **D**, left ilium in ventral view. Arrows indicate dorsal and anterior directions. **Abbreviations**: **a.is**; articulation for the ischium; **a.pu**, articulation for the pubis; **ac**, acetabulum; **cr**, crest; **il**, ilium; **ilb**, iliac blade; **is**, ischium; **isp**, ischiadic peduncle; **prp**, preacetabular process; **pop**, postacetabular process; **pu**, pubis; **pup**, pubic peduncle; **sac**, supraacetabular crest. Scale bars equal 20 mm.

the metacarpal IV and the ulnare. This last one could be the element that Bonaparte (1972) erroneously identified as a possible distal element of the carpus (Fig. 8F–G). Phalanx I-1 is short, wide, and dorsoventrally depressed. The proximal end is more laterally expanded than the distal one, being 1.5 times wider than the latter. Moreover, the proximal end of the phalanx is ventrally expanded, duplicating the height of the shaft. This phalanx also has a lateral pit that is ventrolaterally oriented because of the deformation of the element. Neither extensor nor depressor fossae could be recognized on the dorsal and ventral surfaces of the phalanx (Fig. 8F). The disarticulated phalanx is smaller than phalanx I-1, and only its ventrolateral surface is exposed (Fig. 8G). The proximal end of this phalanx is ventrally expanded, forming two small condyles separated by a proximodistally oriented shallow furrow (Fig. 8G). The anterior end is partially covered and therefore its articular ginglymus cannot be clearly distinguished, although in lateral view it is possible to see that it is anteriorly convex, keeping the same height of the shaft, and it has a small lateral pit (Fig. 8G).

Ilium—This element is better preserved in the referred specimen PVL 3828 of *R. tenuisceps* because the ilium of PVL 3827 suffered some degree of dorsoventral deformation and the iliac blade is incomplete, and that of PVL 3826 only preserved its anterior half. The preacetabular process of the ilium is remarkably short; it curves anterolaterally and thickens anteriorly (Fig. 9A–D). This process does not extend beyond the pubic peduncle but only reaches the level of the anterior margin of the

acetabulum (Fig. 9A–B). The postacetabular process is elongated, duplicating the anteroposterior length of the acetabulum and tapering posteriorly (PVL 3828). It has a well-developed crest on its medial surface that extends anteroventrally to posterodorsally near its ventral margin (Fig. 9B), but no brevis crest or fossa on its lateroventral margin. The iliac blade represents one-third of the height of the ilium and is tilted at 45° from the vertical plane of the iliac body (Fig. 9A, B). The lateral surface of the iliac blade is flat, the medial surface is concave, and the dorsal margin is slightly concave (PVL 3828). There is no vertical ridge or rugosity on the lateral side of the iliac blade of *R. tenuisceps*, unlike in several basal loricatans (e.g., *Batrachotomus kupferzellensis*: SMNS 52970; *Postosuchus kirkpatricki*: TTU-P09002; *Poposaurus gracilis*: UCMP 25962; *Shuvosaurus inexpectatus*: TTU-P09003; *Arizonasaurus babbitti*: Nesbitt, 2005; *Effigia okeeffeae*: Nesbitt, 2007). The pubic process is larger than the ischiadic process and is anteroventrally projected, forming the anterior wall of the acetabulum; it is wide and rounded on its anterior margin. Its articular surface is 'comma'-shaped, being anteriorly convex and posteriorly concave and tapering abruptly into a lamina toward its posteromedial end (Fig. 9A–D). The ischiadic process is dorsoventrally shorter than the pubic one and is ventrally projected, forming the posterior margin of the acetabulum. Its articular surface is 'teardrop'-shaped and ventrally convex (Fig. 9A–D). The acetabular wall is incipiently perforated, as seen in poposauroid and some crocodylomorph pseudosuchians and in avemetatarsalians, differing form the closed acetabular wall seen in
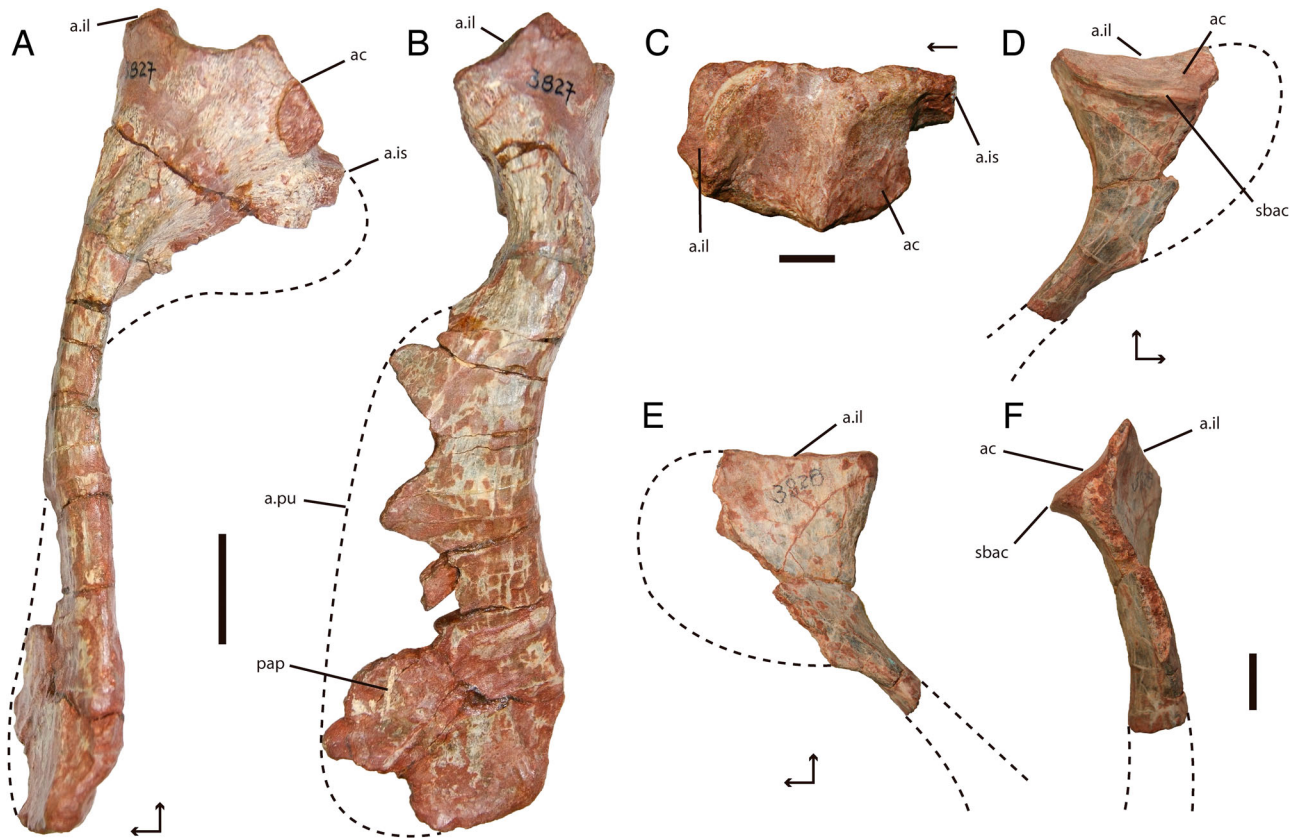
FIGURE 10. Pelvic elements of *Riojasuchus tenuisceps*. Left pubis of PVL 3827 in **A**, lateral, **B**, anterior, and **C**, proximal views; right ischium of PVL 3828 in **D**, lateral, **E**, medial and **F**, anterior views. Arrows indicate dorsal and anterior directions. **Abbreviations**: **a.il**, articulation for the ilium; **a.is**, articulation for the ischium; **a.pu**, articulation for the pubis; **ac**, acetabulum; **pap**, pubic apron; **sbac**, subacetabular crest. Scale bars equal 20 mm (**A–B**) and 10 mm (**C–F**).

most pseudosuchians (aetosaurs, gracilisuchids, erpetosuchids, basal loricatans). The supraacetabular crest of the ilium of *Riojasuchus tenuisceps* is well developed and laterally projecting (Fig. 9A, D) as in most archosauriforms and archosarus, excepting the poposauroids *Effigia okeeffeae*, *Shuvosaurus inexpectatus*, *Poposaurus gracilis*, and *Sillosuchus longicervix*, in which the distal margin of this crest is ventrally projected. The articular surfaces for the sacral ribs are not clearly defined on the medial surface of the ilium, although the crest on the postacetabular process probably defines the ventral margin of the articular surface for the last sacral rib (PVL 3828).

Pubis—The pubis of *R. tenuisceps* is an elongated element that forms a well-expanded pubic apron probably reaching its distal end; however, it cannot be confirmed with certainty whether it contacts its counterpart entirely. The proximal end of the pubis is subtriangular in lateral view, and its proximal margin has two distinguishable articular surfaces: an anterior one for the ilium and a posterior one for the ischium. The articular surface for the ilium occupies the anterior half of the proximal surface of the pubis and is represented by two concavities separated by a marked transversal ridge. Posterior to this area, the proximal region of the pubis has a wide concavity that forms the anteroventral corner of the acetabulum (Fig. 10A–C). The articular surface for the ischium is incomplete but can be identified as a thin, plate-like structure that projects posteriorly from the posteromedial corner of the proximal end of the pubis (Fig. 10A, C). The anterior margin of the proximal end of the pubis has no prepubic process as happens in most archosaurs, excepting ornithischian dinosaurs. The obturator foramen was not preserved on the

pubis of PVL 3827; therefore, its size cannot be determined. The distal two-thirds of the pubis becomes remarkably thin compared with its proximal third; it expands medially and its main axis lateromedially oriented, rotated at ca. 90° from the main axis of the proximal end of the pubis. Therefore, the distal end of the pubis forms a laminar pubic apron that probably contacts its counterpart, but it is not possible to determine with certainty because its medial margin is incomplete (Fig. 10B). The distal end of the pubis of *R. tenuisceps* does not expand anteroposteriorly and therefore does not form a pubic boot like that seen in some derived loricatans (e.g., *Postosuchus kirckpatricki*: Weinbaum, 2013; *Arizonasaurus babbitti*: Nesbitt, 2005; *Poposaurus gracilis*: TMM 43683-1; *Shuvosaurus inexpectatus*: TTU-P18418) and dinosaurs (e.g., *Herrerasaurus ischigualastensis*).

Ischium—The ischium of *R. tenuisceps* is only known for a small fragment of the posterior region of the proximal end (PVL 3828) (Fig. 10D–F). The anteroventral margin is broken, and its contact with the pubis is unclear. The small portion preserved of the anteroventral margin is smooth and concave as in most pseudosuchians, differing from the loricatans *Prestosuchus chiniquensis* (SNSB-BSPG AS XXV, UFRGS-PV-0629T), *Postosuchus kirkpatricki* (TTU-P09002), and *Stagonosuchus nyassicus* (GPIT/RE/3832), which have a notch in the proximal region. The posterior margin of the ischium is complete; it is markedly concave and does not have any tubercle as that seen in *S. nyassicus* (GPIT/RE/3832). The proximal surface of the ischium has a thin articular surface for the ilium on its medial border and a concavity on its lateral side that contributes to the acetabulum (Fig. 10D–F). This region of the acetabulum is
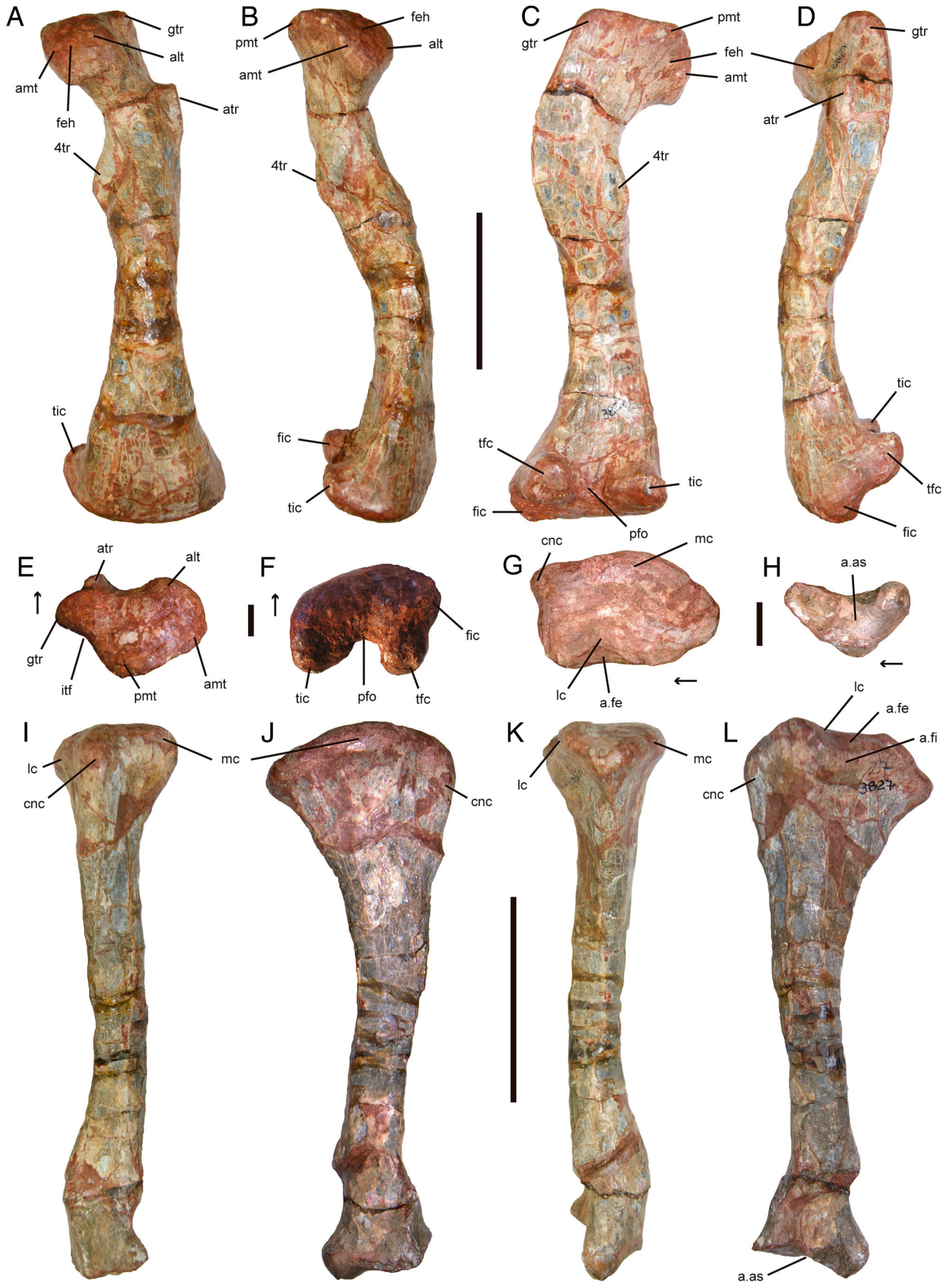
FIGURE 11. Femur and tibia of *Riojasuchus tenuisceps* PVL 3827. **A**, anterior, **B**, medial, **C**, posterior, **D**, lateral, **E**, proximal, and **F**, distal views of left femur; **G**, proximal, **H**, distal, **I**, anterior, **J**, medial, **K**, posterior, and **L**, lateral views of left tibia. Arrows indicate anterior direction. **Abbreviations**: **4tr**, fourth trochanter; **a.as**, articulation for the astragalus; **a.fe**, articulation for the femur; **a.fi**, articulation for the fibula; **alt**, anterolateral tuber; **amt**, anteromedial tuber; **atr**, anterior trochanter; **cnc**, cnemial crest; **feh**, femoral head; **fic**, fibular condyle; **gtr**, greater trochanter; **itf**, intertrochanteric fossa; **lc**, lateral condyle; **mc**, medial condyle; **pfo**, popliteal fossa; **pmt**, posteromedial tuber; **tfc**, tibiofibular crest; **tic**, tibial condyle. Scale bars equal 50 mm (**A–D, I–L**) and 10 mm (**E–H**).

delimitated by a well-developed laterally projected subacetabular crest (Fig. 10D, F). The lateral surface on the proximal end of the ischium of *R. tenuisceps* is concave, whereas the medial surface is completely flat. The distal end of the preserved fragment of the ischium is posterolaterally rotated; therefore, its anteromedial margin would probably reach and contact its counterpart and the posterior margin would diverge from the other.

Femur—The femur of *R. tenuisceps* is sigmoid in posterior view, with it head slightly rotated and anteromedially directed (Fig. 11A–D), but it is not differentiated by any neck, constriction, or flange (PVL 3827, PVL 3828). The proximal surface of the femoral head is convex and does not have a longitudinal furrow as that seen in *Ornithosuchus woodwardi* (NHMUK PV R3561), *Poposaurus gracilis* (TTU-P10419, TMM 31100-408), or *Shuvosaurus inexpectatus* (TTU-P18307, TTU-P18308, TTU-P18309). The main axis of the proximal surface of the femur of *R. tenuisceps* is anteromedially to posterolaterally oriented and is almost twice as long as its perpendicular axis. The anterolateral tuber (sensu Nesbitt, 2011) is rounded and prominent (Fig. 11E); it resembles that of most pseudosuchians, but in dinosauriforms the anterolateral tuber is sharp and forms a crest (Nesbitt, 2011). The anteromedial tuber is globose but not so prominent; it is wide and not clearly separated from the posteromedial tuber; together with the other tubers it lends a subrectangular shape to the proximal end of the femur in proximal view (Fig. 11E). The posteromedial tuber of *R. tenuisceps* is the largest of the proximal tubers; it is well developed and separated from the greater trochanter by a shallow intertrochanteric fossa (= trochanteric fossa sensu Novas, 1996) (Fig. 11E).

The greater trochanter is expanded up to the proximal surface of the femur; it is rounded and thick, being as wide as one-third of the femur head width (PVL 3827) (Fig. 11C–E). The anterior trochanter of *R. tenuisceps* is markedly asymmetric, with its apex toward its proximal end (Fig. 11A, D, E). This trochanter is proximodistally elongated, extending up to the ventral margin of the femoral head and smoothing gradually down into the shaft, resembling that of *Ornithosuchus woodwardi*. This differs from ornithischian and tetanuran dinosaurs, of which the anterior trochanter is partially separated from the shaft (Langer and Benton, 2006; Nesbitt, 2011). The fourth trochanter of the femur of *R. tenuisceps* (PVL 3827, PVL 3828) is elongated, but there are some differences between the two complete femora preserved. In PVL 3827 (Fig. 11A–C), the trochanter is symmetric like in most pseudosuchians and theropod dinosaurs, whereas in the referred specimen, PVL 3828, it is asymmetric, with its apex distally directed as seen in ornithischian and sauropodomorph dinosaurs (Langer and Benton, 2006), a difference that could be a consequence of the stronger taphonomic deformation that affected PVL 3828. The fourth trochanter of *R. tenuisceps* is elongated and extends from the level of the distal margin of the anterior trochanter to the mid-length of the shaft, occupying roughly the proximal second quarter of the femur (Fig. 11A).

The dorsolateral surface of the femur is flat because there is no dorsolateral trochanter on the femur of *R. tenuisceps* (PVL 3827, PVL 3828). The distal end of the femur is expanded, being 2.5 times wider than the shaft, and its anterior surface is flat, without a distinct extensor fossa (Fig. 11A, F). The posterior region of the distal end of the femur has a deep popliteal fossa restricted between the tibial condyle and the tibiofibular crest, which does not extend to the distal surface of the femur (Fig. 11C, F). The tibial condyle is subtringular in distal view, with its apex slightly posteromedially oriented (Fig. 11F). The tibiofibular crest is robust, slightly laterally compressed but with a round edge; it projects posteriorly up to the same level of the tibial condyle (Fig. 11F). In distal view, the tibiofibular crest is slightly narrower than the tibial condyle and half the width of the fibular condyle, with which it forms a wide angle (Fig. 11F). The fibular condyle is rounded and globose and extends distally

further than the tibial condyle (Fig. 11C). The distal surface of the femur is smooth and lacks any furrow between the tibiofibular crest and the fibular condyle, as also happens in phytosaurs, *Revueltosaurus callenderi*, aetosaurs, and *Gracilisuchus stipanicicorum*.

Tibia—The tibia of *R. tenuisceps* is slightly more robust than the fibula; its proximal end is anteroposteriorly expanded, being three times the thickness of the shaft. Its proximal surface is convex, as happens in most archosauriforms. The tibia has a large lateral condyle that, in proximal view, occupies the anterior half of the lateral surface of the tibia (Fig. 11G). The lateral condyle is rounded and has a marked concavity on its proximolateral edge where it articulates proximally with the fibular condyle and the tibiofibular crest of the femur and laterally with the fibula (Fig. 11G, I, K, L). This condition is also present in most pseudosuchians (e.g., *Batrachotomus kupferzellensis*, *Saurosuchus galilei*, *Effigia okeeffeae*, *Hesperosuchus agilis*) but differs from the lateral condyle of the tibia of avemetatarsalians, which does not have said concavity (Nesbitt, 2011). The posterior margin of the proximal end of the tibia of *R. tenuisceps* (PVL 3827, PVL 3828) has a globose medial condyle that is lateromedially half as wide as the proximal end of the tibia (Fig. 11G, I–K). Unlike most archosauriforms and pseudosuchians, the tibia of *R. tenuisceps* has a well-developed cnemial crest on the anteromedial edge of the proximal end of the tibia, which is anteriorly projected (Fig. 11G, I–J, L). It resembles the condition in nondinosaurian dinosauromorphs and proterochampsids in which the cnemial crest is straight; moreover, it differs from dinosaurs because in these the cnemial crest is anterolaterally projected and curved (Nesbitt, 2011). There is no fibular crest on the lateral surface of the tibia as that present in some basal dinosaurs (e.g., *Silesaurus opolensis*: Dzik, 2003; *Sacisaurus agudoensis*: Ferigolo and Langer, 2007; *Saturnalia tupiniquim*: Langer, 2003; *Heterodontosaurus tucki*: Santa Luca, 1980). The shaft of the tibia of *R. tenuisceps* is oval in cross-section, with its main axis anteroposteriorly oriented. The distal end of the tibia is slightly anteroposteriorly expanded and has a thin edge delimiting the articular facet for the astragalus. The lateral surface of the distal end of the tibia is concave, whereas the medial surface is convex (Fig. 11H). The articular facet for the astragalus is concave, and its posterior half is more distally projected than the anterior one (PVL 3827) (Fig. 11H, L).

Fibula—The fibula of *R. tenuisceps* (PVL 3827) is a gracile element, slightly thinner than the tibia. Its proximal end is posteromedially projected, barely laterally expanded, and its articular surface for the femur is flat (Fig. 12A–D). The shaft is anteriorly arched and has a subcircular cross-section. On its anterolateral surface, there is a distinct tubercle for the insertion of the musculus iliofibularis located slightly proximal to the mid-length of the fibula (Fig. 12A–C). This tubercle is elongated, symmetric, laterally compressed, and has a rounded apex, which resembles the condition in phytosaurs and aetosaurs. The distal end of the fibula is slightly anteroposteriorly expanded; its articular surface is gently concave and articulates distally with the calcaneum and medially with the astragalus (Fig. 12A–C, E).

The astragalus and the calcaneum of *R. tenuisceps* form a 'crocodile-reversed' crurotarsan articulation in which the calcaneum has the concavity that holds the condyle of the astragalus (Fig. 13), a condition that is currently only recognized in ornithosuchids.

Astragalus—The astragalus of *R. tenuisceps* (PVL 3827) is an anteroposteriorly compressed and lateromedially elongated element. It articulates ventrally with the metatarsals I and II and the distal tarsal 3, dorsally with the tibia, dorsolaterally with the fibula, and ventrolaterally with the calcaneum (Fig. 13E, F). The anterior surface of the astragalus has a marked central concavity. The posterior surface, on the other hand, is convex on its ventromedial half but has a marked depression on
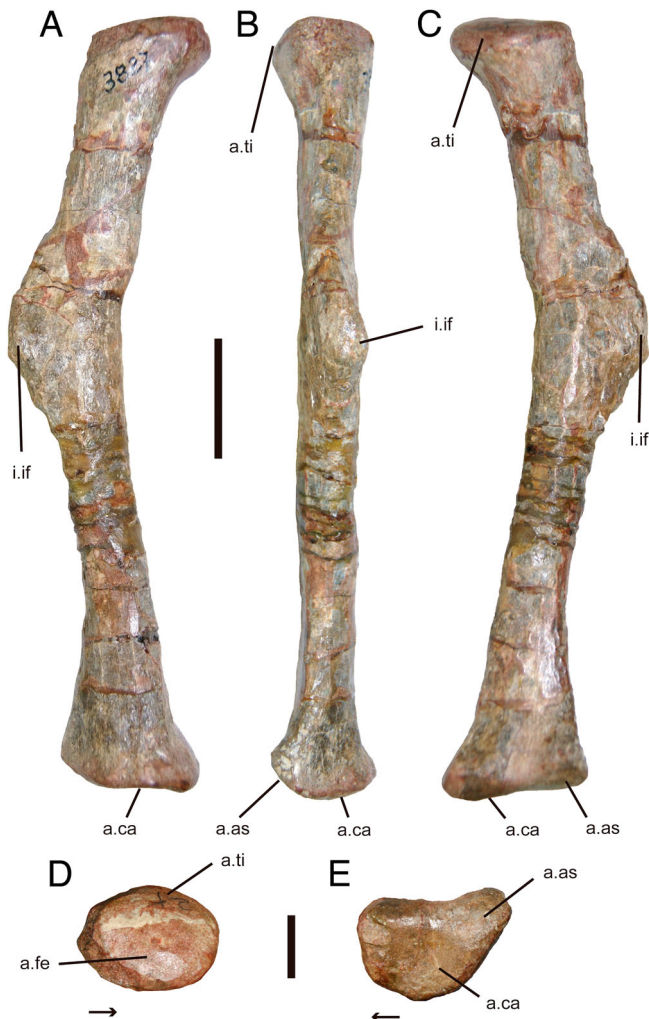
FIGURE 12. Left fibula of *Riojasuchus tenuisceps* PVL 3827 in **A**, lateral, **B**, anterior, **C**, medial, **D**, proximal, and **E**, distal views. Arrows indicate anterior direction. **Abbreviations**: **a.as**, articulation for the astragalus; **a.ca**, articulation for the calcaneum; **a.fe**, articulation for the femur; **a.ti**, articulation for the tibia; **i.if**, insertion for the M. iliofibularis. Scale bars equal 20 mm (**A–C**) and 10 mm (**D–E**).

of *R. tenuisceps* (PVL 3827) extends from the apex of the dorsal process of the astragalus to its lateral edge; it is concave and complements the convex articular surface in the calcaneum (Fig. 13E, F).

Calcaneum—The calcaneum of *R. tenuisceps* (PVL 3827, PVL 3828) has a subtriangular body, in dorsal view, that articulates proximomedially with the astragalus and distally with the distal tarsal 4 (Fig. 13G–I). The lateral third of the proximal surface of the calcaneum forms the articular facet for the fibula; it is convex and anteroposteriorly elongated (Fig. 13G) and is complemented by the articular surface for the fibula on the astragalus (Fig. 13E, F). This condition of the calcaneum resembles that in *Euparkeria capensis* and differs from that in phytosaurs and suchians, in which the articular surface for the fibula is hemicylindrical. The medial two-thirds of the calcaneum of *R. tenuisceps* (PVL 3827, PVL 3828) tapers abruptly to form a medially projected articular condyle. This surface is dorsally and ventrally convex; its dorsal and medial regions articulate with the astragalus, whereas the ventral region articulates with the distal tarsal 4 (Fig. 13G–I). Because of this peculiar tarsal configuration, the articular facet for the astragalus and the one for the fibula form a continuous surface, not separated by any change in slope or ridge (Fig. 13G). This condition differs from that in most pseudosuchians and also differs from the crocodile-reversed tarsus of *Ornithosuchus woodwardi* (NHMUK PV R2410), in which these facets are apparently separated by a strong change of slope.

The lateral surface of the calcaneum has a deep concavity (Fig. 13B). The calcaneal tuber is well developed, as long as the body of the calcaneum, and posterodorsally directed (Fig. 13G–I), differing from *Proterosuchus fergusi*, phytosaurs, and non-crocodylian crocodylomorphs in which the tuber is more posteriorly expanded. Its posterior surface is convex, differing from some aetosaurs (e.g., *Stagonolepis robertsoni*: Walker, 1961) and loricatans (e.g., *Fasolasuchus tenax*: PVL 3850; *Prestosuchus chiniquensis*: SNSB-BSPG AS XXV; *Poposaurus gracilis*: TTM 19886, TMM 31100-378) in which the posterior surface of the calcaneal tuber has a deep dorsoventrally directed furrow. The tuber of *R. tenuisceps* is anteriorly constricted, forming a neck that is lateromedially wider than dorsoventrally high (Fig. 13G–I), similar to that of *Euparkeria capensis*, *Ornithosuchus woodwardi*, and other pseudosuchians. Moreover, the posterior margin of the tuber is expanded on its dorsal, medial, and ventral margins, as also seen in other pseudosuchians (including phytosaurs).

On its ventral surface, the calcaneum of *R. tenuisceps* has a depressed area that separates the articular facet for the distal tarsal 4 from the calcaneal tuber, as also happens in phytosaurs and suchians, but differing from the loricatans *Postosuchus kirkpatricki* and *Prestosuchus chiniquensis* and the crocodylomorphs *Hesperosuchus agilis*, *Dromicosuchus grallator*, *Terrestrisuchus gracilis*, and *Protosuchus richardsoni* in which this depressed area is much deeper, forming a fossa (Nesbitt, 2011).

Distal Tarsals—These are represented by distal tarsals 3 and 4 only; distal tarsals 1 and 2 are either not present or unossified, as suggested for proterochampsids and most archosaurs. Distal tarsals 3 and 4 were preserved in articulation with the astragalus, calcaneum, and metatarsals of the holotype (Figs. 13A, B, 14A, B), and one distal tarsal 4 of PVL 3828 was preserved isolated. Distal tarsal 3 is rectangular, lateromedially compressed, and elongated on its dorsoventral axis. It articulates medially with the metatarsal II, proximally with the metatarsal III, laterally with the distal tarsal 4, and distally with the astragalus (Fig. 14B). Distal tarsal 3 is approximately three times narrower than the distal tarsal 4. This last one is trapezoidal in distal view, and, as happens in archosauriforms and other pseudosuchians, it is lateromedially wider than the distal tarsal 3. Distal tarsal 4 articulates medially with the distal tarsal 3, proximally with the metatarsals III and IV, lateroventrally with the metatarsal V, and dorsodistally with the calcaneum (Figs. 13A, B, 14A, B). In ventral view, the proximal margin of
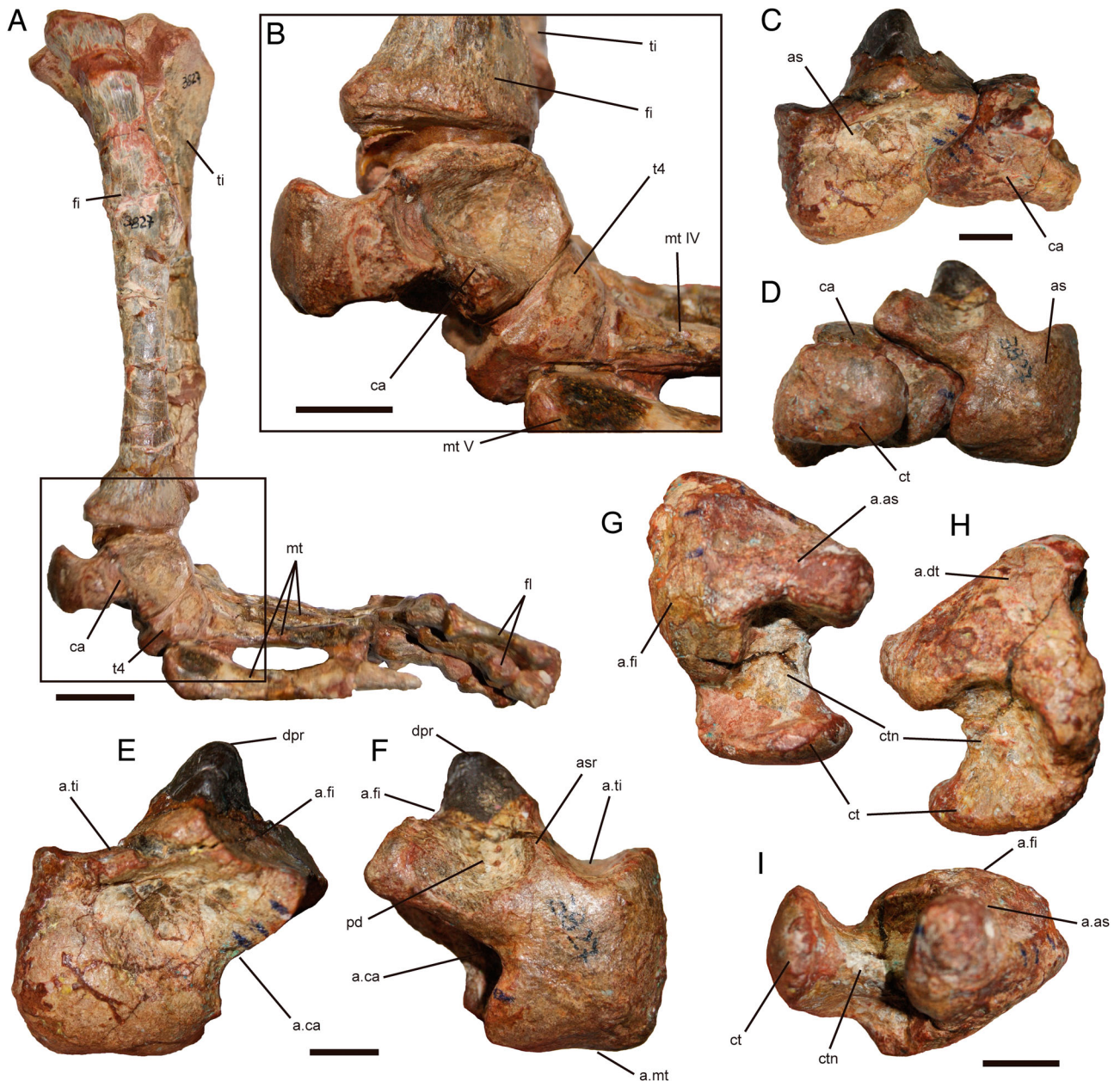
its dorsolateral half. This posterior depression is located between the articular facet for the tibia and that for the fibula and has been identified by Sereno (1991) as homologous to the posterior groove of the astragalus. The posterior groove separates the dorsal from the ventral articular facet of the astragalus, and when articulating with the calcaneum, it forms the astragalocalcanear canal. This posterior groove and astragalocalcanear canal can be seen in other pseudosuchians such as phytosaurs, crocodylians, *Gracilisuchus stipanicicorum*, and *Fasolasuchus tenax*. However, the posterior depression of the astragalus of *R. tenuisceps* (Fig. 13F) does not seem to correspond to the same structure as the posterior groove of other pseudosuchians because it is not located between the same articular facets and does not participate in forming the same anatomical structure: an astragalocalcanear canal. The dorsal process is well developed and anterodorsally directed (Fig. 13E, F). The posteromedial surface of the dorsal process is represented by the articular surface for the tibia, which is concave, medially delimited by a crest, and dorsally restricted by a thick astragalar ridge that projects anterodorsally (Fig. 13E, F). The articular facet for the fibula

FIGURE 13. *Riojasuchus tenuisceps*, tarsal elements of PVL 3827. **A**, right tibia, fibula, tarsus, and pes preserved in articulation; **B**, detail of tarsus in lateral view; **C**, anterior and **D**, posterior views of left astragalus and calcaneum in 'crocodile-reversed' articulation; **E**, anterior and **F**, posterior views of left astragalus; **G**, dorsal, **H**, ventral, and **I**, medial views of left calcaneum. **Abbreviations: a.as**, articulation for the astragalus; **a.ca**, articulation for the calcaneum; **a.dt**, articulation of the distal tarsals; **a.fi**, articulation for the fibula; **a.mt**, articulation for the metatarsals; **a.ti**, articulation for the tibia; **asr**, astragalar ridge; **ca**, calcaneum; **ctn**, calcaneal tuber neck; **dpr**, dorsal process; **fi**, fibula; **mt**, metatarsal; **mt IV**, metatarsal IV; **mt V**, metatarsal V; **pd**, posterior depression; **ti**, tibia; **t4**, distal tarsal 4. Scale bars equal 20 mm (**A**) and 10 mm (**B–I**).

distal tarsal 4 is rounded and the mediodistal corner is more distally projected than the laterodistal one. The proximodorsal surface is convex, whereas the ventrodistal one is concave; the articular surfaces for the calcaneum and the metatarsals are slightly concave.

Pes—Both pedes of *R. tenuisceps* were preserved in PVL 3827 and some isolated phalanges in PVL 3828. The right pes of PVL 3827 has five metatarsals articulated with the complete tarsus and most of the phalanges (Fig. 14A, B), whereas the left pes is only represented by metatarsals I to IV with most of the articulated phalanges. The metatarsals of *R. tenuisceps* become longer from I to IV, whereas metatarsal V is almost as short as metatarsal

I. Metatarsal I is the shortest of the series, and, unlike the other metatarsals, its proximal end is not laterally expanded but instead is dorsoventrally expanded, duplicating the height of the shaft. Metatarsals II to IV are lateromedially expanded on their proximal ends, partially overlapping their medial third over the lateral side of the next one (Fig. 14A, B). This condition can be seen in most basal pseudosuchians, differing from avemetatarsalians and crocodylomorphs (e.g., *Terrestrisuchus gracilis*, *Protosuchus haughtoni*) in which the metatarsus is compact, with metatarsals II to IV overlapping half of their proximal ends (Sereno, 1991; Nesbitt, 2011). Metatarsals I to IV of
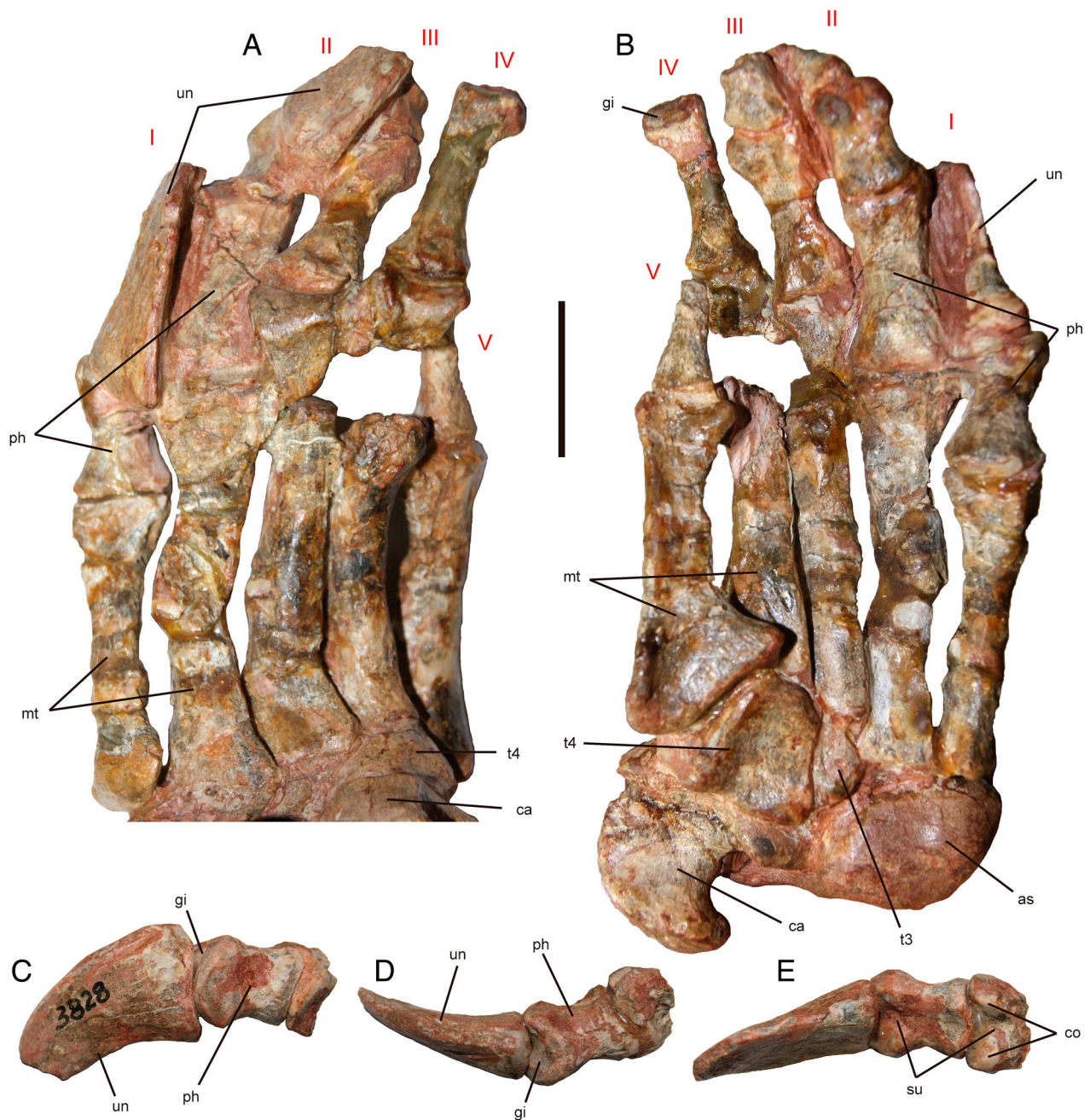
FIGURE 14. *Riojasuchus tenuisceps*, articulated right pes of PVL 3827 in **A**, dorsal and **B**, ventral views; articulated phalanges of PVL 3828 in **C**, lateral, **D**, dorsal, and **E**, ventral views. **Abbreviations**: **as**, astragalus; **ca**, calcaneum; **co**, condyle; **fi**, fibula; **gi**, ginglymus; **mt**, metatarsal; **ph**, phalanx; **su**, sulcus; **t3**, distal tarsal 3; **t4** distal tarsal 4; **un**, unguals. Scale bars equal 20 mm (**A–B**) and 10 mm (**C–E**).

Riojasuchus tenuisceps (PVL 3827) have almost the same diameter. In *R. tenuisceps*, metatarsal IV is the longest of the series but it does not exceed half the length of the tibia. Lastly, metatarsal V is the most robust of the series; its proximal end is medially expanded, giving it a 'hook' shape. The proximal surface of this medial projection forms an acute angle of 65° with the main axis of the metatarsal (Fig. 14A, B). Metatarsal V is subparallel to the other metatarsals in *R. tenuisceps*, as also seen in some pseudosuchians such as *Parasuchus hislopi*, *Neoaetosauroides engaeus*, *Stagonolepis robertsoni*, and *Gracilisuchus stipanicicorum*, but differing from the divergent metatarsal V of

Euparkeria capensis, *Ticinosuchus ferox*, and *Saurosuchus galilei* (Lecuona and Desojo, 2011).

The pedal phalanges of *Riojasuchus tenuisceps* are partially preserved, and although Bonaparte (1972) proposed a phalangeal formula of 2-3-4-4?-2?, this cannot be determined with certainty beyond a 2-3-2+-1+-1 formula. Digits I, II, and V were preserved complete in PVL 3827; the ungual of the first digit is larger than that of the second digit, and the phalanx corresponding to the fifth digit is reduced (Fig. 14A, B). On the preserved digits with more than one phalanx, it can be observed that the more distal phalanges are remarkably longer than the

proximal ones; the longest one known is on digit IV, which is as long as half its corresponding metatarsus. The non-ungual phalanges of *R. tenuisceps* have both the proximal and distal ends dorsoventrally expanded, and the shafts are circular in cross-section. The proximal articular surface of the phalanges is concave and articulates with the corresponding metatarsal or proximal phalanx. The distal articular surface is a convex ginglymus articulation that is slightly dorsoventrally higher than the proximal end and articulates with the following phalanx (Fig. 14C–E). The ventral surface of the distal end of the phalanges has an anteroposteriorly oriented furrow that separates it into two small elliptic condyles (Fig. 14C–E). The lateral surfaces, on the other hand, have a very slight lateral depression on each side that probably corresponds to the lateral pits, but the lateral surfaces were overprepared and the nature of the depression is difficult to determine. The phalanx of the fifth digit is remarkably different in morphology from the rest of the phalanges. It is reduced to an almost conical structure, and its proximal surface is smaller than that of the other pedal phalaxes. The preserved ungual phalanges of *R. tenuisceps* correspond to the digits I and II of PVL 3827 and some isolated ones of PVL 3828 (Fig. 14A–E). These are anteroventrally curved, laterally compressed, dorsoventrally high, even duplicating the height of their previous phalanx (Fig. 14C–E), and also longer than said phalanx. Their lateral surfaces are smooth, and the dorsal and ventral margins taper, forming edges.

DISCUSSION

Osteology

Numerous features recognized on the postcranial skeleton of *Riojasuchus tenuisceps* were quite remarkable when compared with other pseudosuchians and are discussed below.

Concerning the axial skeleton of *R. tenuisceps*, the development of cervical ventral keels and spine tables is noteworthy, as well as the absence of laminae and fossae in all regions of the axial skeleton and the presence of three sacral vertebrae. Cervical vertebrae have a ventral keel that extends ventral to the centrum rim. This condition is quite common among archosauromorphs such as erythrosuchids (e.g., *Erythrosuchus africanus* and *Garjainia prima*) and proterochampsids (e.g., *Proterochampsa barrionuevoi*, *Tropidosuchus romeri*, *Gualosuchus reigi*, *Chanaresuchus bonapartei*), but somewhat rare within pseudosuchians in which it can only be recognized in erpetosuchids (*Erpetosuchus granti* and *Tarjadia ruthae*), the aetosaur *Stagonolepis robertsoni*, and the loricatan *Batrachotomus kupferzellensis*.

On the other hand, spine tables are only present on the cervical vertebrae of *R. tenuisceps* and the rest of the axial skeleton has laterally compressed neural spines. These cervical spine tables are laterally expanded in their middle region, conferring them a suboval or subrectangular shape in dorsal view, as occurs in *Ornithosuchus woodwardi* (NHMUK PV R3916), *Euparkeria capensis* (Ewer, 1965), *Tarjadia ruthae* (CRILAR-Pv 478), *Parringtonia gracilis* (NHMUK PV R8646), *Erpetosuchus granti* (Benton and Walker, 2002), and some phytosaurs. These cervical vertebrae differ from those of several loricatans (*Postosuchus kirkpatricki*: TTU-P09235; *Saurosuchus galilei*: PVL 2198; *Batrachotomus kupferzellensis*: SMNS 80285-92) and *Nundasuchus songeaensis*, in which the neural spines are laterally expanded only on their anterior end, giving it a subtriangular shape in dorsal view. In the phylogenetic analyses of Lacerda et al. (2018) and Ezcurra et al. (2017), *R. tenuisceps* (PVL 3827), *Ornithosuchus woodwardi* (NHMUK PV R3916), and *Gracilisuchus stipanicicorum* (Lecuona et al., 2017) were scored as having spine tables on the dorsal vertebrae, but they only have spine tables on their cervical vertebrae, so it is here recommended to

score them as 'spine tables absent' in future matrices (see Appendices 1, 2 in Supplemental Data 1). This was corrected in the phylogenetic revision of the latest matrices of Ezcurra et al. (2017) and Lacerda et al. (2018), which were discussed in the present contribution, but did not affect the relationships of said taxa.

The presence of three sacral vertebrae in *Riojasuchus tenuisceps* differs from basal archosauriforms and most pseudosuchians, which keep the plesiomorphic condition of having two sacral vertebrae. Only the rauisuchian *Batrachotomus kupferzellensis* (SMNS 80298), poposauroids (*Arizonasaurus babbitti*: Nesbitt, 2005; *Poposaurus gracilis*: TMM 43683-1, UCMP 78719; *Shuvosaurus inexpectatus*: TTU-P09001), and the ornithosuchids *Ornithosuchus woodwardi* (Walker, 1964) and *Riojasuchus tenuisceps* have three sacral vertebrae, which is here interpreted as independently acquired features in these three groups.

The perforated acetabulum and the anteromedially rotated proximal end of the femur are characters that have been typically regarded as diagnostic for dinosaurs (Gauthier, 1986; Novas, 1996; Ezcurra, 2006; Langer et al., 2010). Because of the presence of these same features in the ornithosuchids *R. tenuisceps* and *O. woodwardi*, a close affinity has been proposed between ornithosuchids and dinosaurs, supporting the group 'Ornithosuchia' (Gauthier, 1986; Benton and Clark, 1988; Bennett, 1996, 2012). However, the perforated acetabulum, defined by the concave ventral margin of the ilium (Nesbitt, 2011:char. 273; Ezcurra et al., 2017:char. 455), has also been registered in other pseudosuchians (poposauroids and crocodylomorphs); thus, it cannot be considered exclusively to be a dinosaurian feature. On the other hand, the anteromedially rotated head of the femur, evaluated as the orientation of the femoral head relative to the shaft (Nesbitt, 2011:char. 305; Ezcurra et al., 2017:char. 493), is in fact a widespread condition that can be registered in numerous archosauriforms, including proterochampsids, pseudosuchians, pterosaurs, and dinosauriforms. The majority of recent phylogenetic analyses (Benton and Walker, 2002; Brusatte et al., 2010; Nesbitt, 2011; Butler et al., 2014; Ezcurra et al., 2017) strongly support the inclusion of ornithosuchids within Pseudosuchia; therefore, those characters would be considered to be convergences between ornithosuchids and dinosaurs. Following the topology presented by Ezcurra et al. (2017), the perforated acetabulum was independently acquired at least four times within Archosauria, and the rotated head of the femur would be a plesiomorphic condition for Archosauriformes.

Probably the most controversial feature present in ornithosuchids is their tarsal morphology. As previously described, this clade has a crocodile-reversed ankle joint, which is a unique condition among archosaurs. This particular condition has stimulated different evolutionary hypotheses in the past decades. Sereno and Arcucci (1990) discussed in detail the relationships among 'crocodile-reversed' (ornithosuchids), 'crocodile-normal' (other pseudosuchians), and 'mesotarsal' (avemetatarsalians) archosaurs. They rebutted the monophyly of the clade 'Ornithosuchia,' which grouped ornithosuchids with avemetatarsalians, because the synapomorphies proposed for the latter group were found to be ambiguous. Subsequently, numerous studies agreed with that rebuttal and presented ornithosuchids within the clade Pseudosuchia (Sereno, 1991; Benton and Walker, 2002; Brusatte et al., 2010; Nesbitt, 2011; Ezcurra, 2016). In this context, the similarities between the tarsus of ornithosuchids and that of the rest of the pseudosuchians became clearer. Both 'crocodile-reversed' and 'crocodile-normal' tarsi have unfused proximal tarsals (astragalus and calcaneum) that articulate freely with each other (Nesbitt, 2011:char. 370; Ezcurra et al., 2017:char. 532). Moreover, another similarity of the calcaneum of ornithosuchids to that of the rest of pseudosuchians (including phytosaurs) is the presence of a well-developed posterior tuber (Nesbitt, 2011:chars. 373, 374) and a convex articular surface for the fibula.
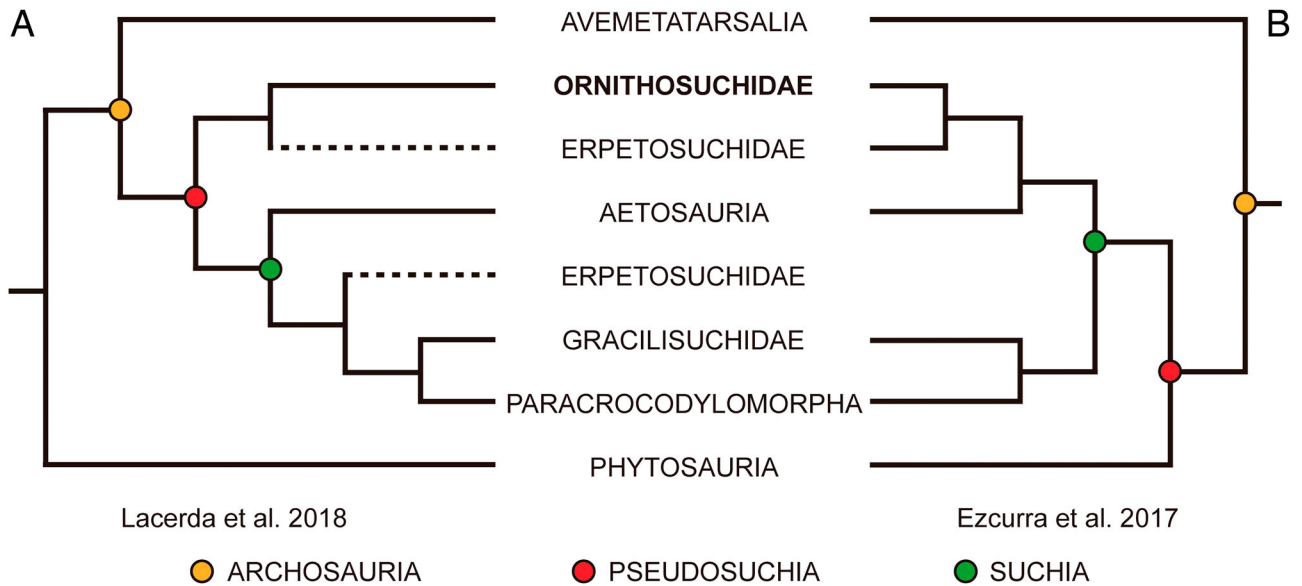
FIGURE 15. Phylogenetic positions of Ornithosuchidae in consensus trees presented by **A**, Lacerda et al. (2018) and **B**, Ezcurra et al. (2017). Dotted lines indicate the possible positions of Erpetosuchidae in Lacerda et al. (2018).

Phylogenetic Position

The latest phylogenetic analysis carried out by Lacerda et al. (2018) incorporated subsequent modifications applied to the data matrix of Nesbitt (2011) (Butler et al., 2011, 2014; Nesbitt and Butler, 2012; Baczko et al., 2014). In this study, Ornithosuchidae was recovered in a clade together with Erpetosuchidae in some (but not all) of the most parsimonious trees. In the remaining trees, Erpetosuchidae was recovered as sister group of Gracilisuchidae + Paracrocodylomorpha (Fig. 15A). In this analysis, Erpetosuchidae was represented only by three species, *Pagosvenator candelariensis*, *Erpetosuchus grantii*, and *Parringtonia gracilis*, which are known from incomplete specimens and, despite grouping together, did not provide stability in the resulting topologies. Therefore, the results of the phylogenetic analysis of Lacerda et al. (2018) suggested a possible close affinity between Ornithosuchidae and Erpetosuchidae, but further studies are required for clarification. On the other hand, the phylogenetic analysis presented by Ezcurra et al. (2017) based on a modification of the data matrix of Ezcurra (2016) helped support the hypothesis of a monophyletic clade that nested Ornithosuchidae and Erpetosuchidae together (Fig. 15B). In the study of Ezcurra et al. (2017), the position of Erpetosuchidae was more stable than in the analysis of Lacerda et al. (2018) owing to the addition of *Tarjadia ruthae*, *Dyoplax arenaceus*, and *Archeopelta arborensis*. These taxa, particularly *Tarjadia ruthae*, provided crucial information about the complete anatomy of erpetosuchids, and consequently their phylogenetic position as sister group of ornithosuchids. Furthermore, the phylogenetic relationships of Ornithosuchidae are currently under revision, with the incorporation of a new key specimen from Brazil (M.B.v.B., pers. observ.). This revision will focus on the internal relationships of this clade and among pseudosuchians; therefore, these are not discussed here.

Histogenesis

Several ossification mechanisms for osteoderms of extinct and extant reptiles have been proposed. The most common mechanism among these taxa is metaplasic ossification (Haines and Mohuiddin, 1968). In this process, the ossification occurs on a different tissue (e.g., tendinous tissue), which transforms into bone tissue. Metaplasic ossification in osteoderms can be identified by the presence of bundles of mineralized collagen, which represents the primary (unmineralized) tissue and interweave in different orientations (i.e., structural fibers; Scheyer and Sander, 2004, 2007; Main et al., 2005; Witzmann and Soler-Gijón, 2008; Cerda and Powell, 2010). Intramembranous ossification is another type of ossification mechanism. This process includes a periosteal layer replacing existing non-cartilage connective tissue. This mechanism is recognized by the absence of structural fibers. A third process of ossification is present only in placodont osteoderms and consists of the formation of osseous tissue from a fibrocartilaginous precursor tissue (Scheyer, 2007). Finally, bone histology reveals that osteoderms of some taxa are formed by a combination of more than one kind of ossification process. For example, although the main ossification process in aetosaurs and *Vancleavea campi* appears to be intramembranous, in some cases structural fibers from the dermis are incorporated to the element later during the ontogeny (Ponce et al., 2017; Cerda et al., 2018).

Following this line of reasoning, intramembranous ossification is proposed to be the main mechanism of osteoderm formation in *Riojasuchus tenuisceps*, because of the absence of structural fibers. However, an early metaplasic process cannot be discarded entirely. This is because abundant primary tissue has been remodeled, and it is possible that structural fibers could have been resorbed during the first stages of osteoderm formation. In a phylogenetic context, for pseudosuchians, the intramembranous ossification seen in *R. tenuisceps* appears to be a plesiomorphic condition. Also, this mechanism is commonly observed in early stages of ontogeny in pseudosuchian osteoderms, including aetosaurs (Cerda and Desojo, 2011; Scheyer et al., 2014; Cerda et al., 2018), *Revueltosaurus callenderi* (Scheyer et al., 2014), and erpetosuchids and proterochampsids (Scheyer et al., 2014; Cerda et al., 2015a; Ponce et al., 2017). The metaplasic ossification has a scarce and patchy distribution among pseudosuchians, including crocodylians, some phytosaurs, and loricatans (e.g.,

Vickaryous and Hall, 2008; Scheyer and Desojo, 2011; Scheyer et al., 2014).

Skeletochronology

Growth marks (i.e., annuli and LAGs) within the osteodermal tissues indicate a slowdown or a complete interruption of bone deposition during the growth of the individual. Because the formation of these growth marks correspond with annual cycles, they have been used to estimate relative or absolute age in extinct and extant tetrapod osteoderms (e.g., Erickson and Brochu, 1999; Ricqlès et al., 2003; Hill and Lucas, 2006; Parker et al., 2008; Witzmann and Soler-Gijón, 2008; Hill, 2010; Scheyer and Sander, 2009; Witzmann, 2009, 2010; Cerda and Desojo, 2011; Scheyer and Desojo, 2011; Taborda et al., 2013; Scheyer et al., 2014; Cerda et al., 2015b; Ponce et al., 2017). Considering our sample, the estimated minimum age at death for *Riojasuchus tenuisceps* (PVL 3814) is three years of age. Nevertheless, because of the prevalence of secondarily formed cancellous bone, it is more likely that most growth lines have been eroded due to the remodeling process. Thus, the number of growth lines, and therefore the age of specimen at death, is possible highly underestimated (Ponce et al., 2019). When compared with other pseudosuchians, such as aetosaurs (e.g., *Aetosauroides scagliai*) and erpetosuchids (e.g., *Archeopelta arborensis*, *Tarjadia ruthae*), osteoderms appear not to be useful for skeletochronological studies in *Riojasuchus tenuisceps* due to its high grade of bone remodeling. In aetosaurs and erpetosuchids, the growth lines are conserved mainly in the basal cortex, which is formed by primary bone (Cerda and Desojo, 2011; Taborda et al., 2013; Cerda et al., 2015a; Ponce et al., 2017). On the other hand, and opposed to what is observed in most pseudosuchians, from a qualitative point of view, the osteoderms of *Riojasuchus tenuisceps* show less compact bone and the internal region of cancellous bone is more extensive. Osteoderms of pseudosuchians and basal archosauriforms (e.g., aetosaurs, erpetosuquids, proterochampsids) are, in general, highly compacted (e.g., Ponce et al., 2017; Cerda et al., 2018).

CONCLUSIONS

We provide a detailed osteological description of the postcranial skeleton ornithosuchid *Riojasuchus tenuisceps*. This species is represented by almost complete specimens with excellent three-dimensional preservation and could be considered to be the best representative of Ornithosuchidae regarding the knowledge of its morphology to date. Its osteological revision evidenced some remarkable features on its skeleton, such as the cervical vertebrae morphology (well-developed table spines and ventral keels), the number of sacral vertebrae, the morphology of the pelvic girdle (perforated acetabulum, elongated pubis), femur (anteromedially rotated head, well-developed anterior trochanter), and astragalus (only known in *Riojasuchus* within Ornithosuchidae), and the 'crocodile-reversed' ankle joint. The latter being a synapomorphic condition of ornithosuchids that is still key for understanding the early evolution of pseudosuchians. The histological analysis performed on its osteoderms provided novel information about its microstructure showing the typical pseudosuchian trilaminar structure with a very extensive internal region of cancellous bone. Intramembranous ossification is proposed to be the main mechanism of osteoderm formation, which seems to be a plesiomorphic condition for pseudosuchians, also known in phytosaurs, some loricatans, and crocodylians. A minimum age of three years can be inferred for the specimen PVL 3814; however, osteoderms of *Riojasuchus tenuisceps* proved to be not useful for skeletochronological studies due to the high degree of bone remodeling.

This detailed revision of the postcranial skeleton of *Riojasuchus tenuisceps* will provide essential information for further studies and will hopefully be useful as a database on ornithosuchid anatomy for comparative purposes and future phylogenetic studies. Moreover, the information provided here will be fundamental to testing hypotheses on the paleobiology of this group, namely, to test whether the postcranial information supports the hypothesis based on cranial biomechanics that implied ornithosuchids occupied scavenger niches in the Triassic continental communities of Pangea.

ORCID

M. Belén von Baczko http://orcid.org/0000-0003-2570-3418
Julia B. Desojo http://orcid.org/0000-0002-2739-3276

LITERATURE CITED

Arcucci, A. B., C. A. Marsicano, and A. T. Caselli. 2004. Tetrapod association and palaeoenvironment of the Los Colorados Formation (Argentina): a significant sample from Western Gondwana at the end of the Triassic. Geobios 37:557–568.

Baczko, M. B. von. 2018. Rediscovered cranial material of *Venaticosuchus rusconii* enables the first jaw biomechanics in Ornithosuchidae (Archosauria: Pseudosuchia). Ameghiniana 55:365–380.

Baczko, M. B. von, and J. B. Desojo. 2016. Cranial anatomy and palaeoneurology of the archosaur *Riojasuchus tenuisceps* from the Los Colorados Formation, La Rioja, Argentina. PLoS ONE 11: e0148575.

Baczko, M. B. von, and M. D. Ezcurra. 2013. Ornithosuchidae: a group of Triassic archosaurs with a unique ankle joint; pp. 187–202 in S. J. Nesbitt, J. B. Desojo, and R. B. Irmis (eds.), Anatomy, Phylogeny, and Palaeobiology of Early Archosaurs and Their Kin. Special Publication 379. Geological Society, London.

Baczko, M. B. von, and M. D. Ezcurra. 2016. Taxonomy of the archosaur *Ornithosuchus*: reassessing *Ornithosuchus woodwardi* Newton, 1894 and *Dasygnathoides longidens* (Huxley, 1877). Earth and Environmental Science Transactions of the Royal Society of Edinburgh 106:199–205.

Baczko, M. B. von, J. B. Desojo, and D. Pol. 2014. Anatomy and phylogenetic position of *Venaticosuchus rusconii* Bonaparte, 1970 (Archosauria, Pseudosuchia), from the Ischigualasto Formation (Late Triassic), La Rioja, Argentina. Journal of Vertebrate Paleontology 34:1342–1356.

Bennett, S. C. 1996. The phylogenetic position of the Pterosauria within the Archosauromorpha. Zoological Journal of the Linnean Society 118:261–308.

Bennett, S. C. 2012. The phylogenetic position of the Pterosauria within the Archosauromorpha re-examined. Historical Biology 25:545–563.

Benton, M. J. 1983. The Triassic reptile *Hyperodapedon* from Elgin: functional morphology and relationships. Philosophical Transactions of the Royal Society of London B: Biological Sciences 302:605–718.

Benton, M. J., and J. M. Clark. 1988. Archosaur phylogeny and the relationships of the Crocodylia; pp. 295–338 in M. J. Benton (ed.), The Phylogeny and Classification of the Tetrapods 1, Amphibians, Reptiles, Birds. Oxford University Press, Oxford, U.K.

Benton, M. J., and A. D. Walker. 2002. *Erpetosuchus*, a crocodile-like basal archosaur from the Late Triassic of Elgin, Scotland. Zoological Journal of the Linnean Society 136:25–47.

Bonaparte, J. F. 1967. Dos nuevas "faunas" de reptiles triásicos de Argentina; pp. 283–325 in A. J. Amos (ed.), Gondwana Stratigraphy, International Union of Geological Sciences Symposium. Asociación Geológica Argentina, 1–15 October 1967, Buenos Aires.

Bonaparte, J. F. 1972. Los tetrápodos del sector superior de la Formación Los Colorados, La Rioja, Argentina. (Triásico Superior) I Parte. Opera Lilloana 22:13–56.

Bonaparte, J. F. 1973. Edades/réptil para el Triásico de Argentina y Brasil; pp. 93–129 in Actas V Congreso Geológico Argentino Vol. 3. Asociación Geológica Argentina, 22-28 October, 1972, Villa Carlos Paz, Buenos Aires.

Brusatte, S. L., M. J. Benton, J. B. Desojo, and M. C. Langer. 2010. The higher-level phylogeny of Archosauria (Tetrapoda: Diapsida). Journal of Systematic Palaeontology 8:3–47.

Butler, R. J., S. L. Brusatte, M. Reich, S. J. Nesbitt, R. R. Schoch, and J. J. Hornung. 2011. The sail-backed reptile *Ctenosauriscus* from the latest Early Triassic of Germany and the timing and biogeography of the early archosaur radiation. PLoS ONE 6:e25693.

Butler, R. J., C. Sullivan, M. D. Ezcurra, J. Liu, A. Lecuona, and R. B. Sookias. 2014. New clade of enigmatic early archosaurs yields insights into early pseudosuchian phylogeny and the biogeography of the archosaur radiation. BMC Evolutionary Biology 14:128.

Cerda, I. A., and J. B. Desojo. 2011. Dermal armour histology of aetosaurs (Archosauria: Pseudosuchia), from the Upper Triassic of Argentina and Brazil. Lethaia 44:417–428.

Cerda, I. A., and J. E. Powell. 2010. Dermal armor histology of *Saltasaurus loricatus*, an Upper Cretaceous sauropod dinosaur from Northwest Argentina. Acta Palaeontologica Polonica 55:389–398.

Cerda, I. A., J. B. Desojo, and T. M. Scheyer. 2015a. Osteoderm histology of Proterochampsia and Doswelliidae (Reptilia: Archosauriformes) and their evolutionary and paleobiological implications. Journal of Morphology 276:385–402.

Cerda, I. A., J. B. Desojo, and T. M. Scheyer. 2018. Novel data on aetosaur (Archosauria, Pseudosuchia) osteoderm microanatomy and histology: palaeobiological implications. Palaeontology 61:721–745.

Cerda, I. A., G. A. Casal, R. D. Martinez, and L. M. Ibiricu. 2015b. Histological evidence for a supraspinous ligament in sauropod dinosaurs. Royal Society Open Science 2:150369.

Chinsamy, A., and M. A. Raath. 1992. Preparation of fossil bone for histological examination. Palaeontologia Africana 29:39–44.

Colbert, E. H. 1952. A pseudosuchian reptile from Arizona. Bulletin of the American Museum of Natural History 99:565–592.

Colbert, E. H., and C. C. Mook. 1951. The ancestral crocodilian *Protosuchus*. Bulletin of the American Museum of Natural History 97:147–182.

Coombs, W. P., Jr. 1995. Ankylosaurian tail clubs of middle Campanian to early Maastrichtian age from western North America, with description of a tiny club from Alberta and discussion of tail orientation and tail club function. Canadian Journal of Earth Sciences 32:902–912.

Cope, E. D. 1869. Synopsis of the extinct Batrachia and Reptilia of North America. Transactions of the American Philosophical Society 14:1–252.

Dzik, J. 2003. A beaked herbivorous archosaur with dinosaur affinities from the early Late Triassic of Poland. Journal of Vertebrate Paleontology 23:556–574.

Erickson, G. M., and C. A. Brochu. 1999. How the 'terror crocodile' grew so big. Nature 398:205–206.

Ezcurra, M. D. 2006. A review of the systematic position of the dinosauriform archosaur *Eucoelophysis baldwini* Sullivan and Lucas, 1999 from the Upper Triassic of New Mexico, USA. Geodiversitas 28:649–684.

Ezcurra, M. D. 2016. The phylogenetic relationships of basal archosauromorphs, with an emphasis on the systematics of proterosuchian archosauriforms. PeerJ 4:e1778.

Ezcurra, M. D., L. E. Fiorelli, A. G. Martinelli, S. Rocher, M. B. von Baczko, M. Ezpeleta, J. R. A. Taborda, E. M. Hechenleitner, M. J. Trotteyn, and J. B. Desojo. 2017. Deep faunistic turnovers preceded the rise of dinosaurs in southwestern Pangaea. Nature Ecology and Evolution 1:1477.

Ewer, R. F. 1965. The anatomy of the thecodont reptile *Euparkeria capensis* Broom. Philosophical Transactions of the Royal Society London B: Biological Sciences 248:379–435.

Ferigolo, J., and M. C. Langer. 2007. A Late Triassic dinosauriform from south Brazil and the origin of the ornithischian predentary bone. Historical Biology 19:23–33.

Forster, C. A. 1990. The postcranial skeleton of the ornithopod dinosaur *Tenontosaurus tilletti*. Journal of Vertebrate Paleontology 10:273–294.

Francillon-Vieillot, H., V. de Buffrénil, J. D. Castanet, J. Géraudie, F. J. Meunier, J. Y. Sire, L. Zylberberg, and A. de Ricqlès. 1990. Microstructure and mineralization of vertebrate skeletal tissues. Skeletal biomineralization: patterns, processes and evolutionary trends 1:471–530.

Gauthier, J. 1986. Saurischian monophyly and the origin of birds. Memoirs of the California Academy of Sciences 8:1–55.

Gauthier, J., and K. Padian. 1985. Phylogenetic, functional, and aerodynamic analyses of the origin of birds and their flight; pp. 185–197 in M. K. Hecht, J. H. Ostrom, G. Viohl, and P. Wellnhofer (eds.), The Beginning of Birds. Freunde des Jura Museums, Eichstatt, Germany.

Gower, D. J. 2003. Osteology of the early archosaurian reptile *Erythrosuchus africanus*, Broom. Annals of the South African Museum 110:1–88.

Haines, R. W., and A. Mohuiddin. 1968. Metaplastic bone. Journal of Anatomy 103:527–538.

Hill, R. V. 2010. Osteoderms of *Simosuchus clarki* (Crocodyliformes: Notosuchia) from the Late Cretaceous of Madagascar. Journal of Vertebrate Paleontology 30:154–176.

Hill, R. V., and S. G. Lucas. 2006. New data on the anatomy and relationships of the Paleocene crocodilian *Akanthosuchus langstoni*. Acta Palaeontologica Polonica 51:455–464.

Huene, F. von. 1908. Die Dinosaurier der europäischen Triasformation mit Berticksichtigung der aussereuropäischen Vorkomnisse. Geologische und Palaeontologische Abhandlungen 1:1–419.

Kent, D. V., P. S. Malnis, C. E. Colombi, O. A. Alcober, and R. N. Martínez. 2014. Age constraints on the dispersal of dinosaurs in the Late Triassic from magnetochronology of the Los Colorados Formation (Argentina). Proceedings of the National Academy of Sciences of the United States of America 111:7958–7963.

Lacerda, M. B., M. A. De Franca, and C. L. Schultz. 2018. A new erpetosuchid (Pseudosuchia, Archosauria) from the Middle-late Triassic of Southern Brazil. Zoological Journal of the Linnean Society, 184 (3):804–824.

Langer, M. C. 2003. The pelvic and hindlimb anatomy of the stem-sauropodomorph *Saturnalia tupiniquim* (Late Triassic, Brazil). PaleoBios 23:1–40.

Langer, M. C., and M. J. Benton. 2006. Early dinosaurs: a phylogenetic study. Journal of Systematic Palaeontology 4:309–358.

Langer, M. C., M. D. Ezcurra, J. S. Bittencourt, and F. E. Novas. 2010. The origin and early evolution of dinosaurs. Biological Reviews 85:55–110.

Lautenschlager, S., and J. B. Desojo. 2011. Reassessment of the Middle Triassic rauisuchian archosaurs *Ticinosuchus ferox* and *Stagonosuchus nyassicus*. Paläontologische Zeitschrift 85:357–381.

Lecuona, A., and J. B. Desojo. 2011. Hind limb osteology of *Gracilisuchus stipanicicorum* (Archosauria: Pseudosuchia). Earth and Environmental Science Transactions of the Royal Society of Edinburgh 102:105–128.

Lecuona, A., J. B. Desojo, and D. Pol. 2017. New information on the postcranial skeleton of *Gracilisuchus stipanicicorum* (Archosauria: Suchia) and reappraisal of its phylogenetic position. Zoological Journal of the Linnean Society 181:638–677.

Main, R. P., A. de Ricqlès, J. R. Horner, and K. Padian. 2005. The evolution and function of thyreophoran dinosaur scutes: implications for plate function in stegosaurs. Paleobiology 31:291–314.

Nesbitt, S. J. 2005. Osteology of the Middle Triassic pseudosuchian archosaur *Arizonasaurus babbitti*. Historical Biology 17:19–47.

Nesbitt, S. J. 2007. The anatomy of *Effigia okeeffeae* (Archosauria, Suchia), theropod-like convergence, and the distribution of related taxa. Bulletin of the American Museum of Natural History 2007:1–85.

Nesbitt, S. J. 2011. The early evolution of archosaurs: relationships and the origin of major clades. Bulletin of the American Museum of Natural History 352:1–292.

Nesbitt, S. J., and R. J. Butler. 2012. Redescription of the archosaur *Parringtonia gracilis* from the Middle Triassic Manda Beds of

Tanzania, and the antiquity of Erpetosuchidae. Geological Magazine 150:225–238.

Novas, F. E. 1996. Dinosaur monophyly. Journal of Vertebrate Paleontology 16:723–741.

Organ, C. L. 2006. Thoracic epaxial muscles in living archosaurs and ornithopod dinosaurs. Anatomical Record Part A: Discoveries in Molecular, Cellular, and Evolutionary Biology 288:782–793.

Parker, W. G. 2005. A new species of the Late Triassic aetosaur *Desmatosuchus* (Archosauria: Pseudosuchia). Comptes Rendus Palevol 4:327–340.

Parker, W. G., M. R. Stocker, and R. B. Irmis. 2008. A new desmatosuchine aetosaur (Archosauria: Suchia) from the Upper Triassic Tecovas Formation (Dockum Group) of Texas. Journal of Vertebrate Paleontology 28:692–701.

Ponce, D. A., I. A. Cerda, J. B. Desojo, and S. J. Nesbitt. 2017. The osteoderm microstructure in doswelliids and proterochampsids and its implications for palaeobiology of stem archosaurs. Acta Palaeontologica Polonica 62:819–831.

Ponce, D. A., M. B. von Baczko, I. A. Cerda, and J. B. Desojo. 2019. Análisis de la morfología y microestructura de osteodermos de *Riojasuchus tenuisceps* (Archosauria: Ornithosuchidae): inferencias paleobiológicas. PE-APA 19(2):Supp R32.

Ricqlès, A. de, K. Padian, and J. R. Horner. 2003. On the bone histology of some Triassic pseudosuchian archosaurs and related taxa. Annales de Paléontologie 89:67–101.

Santa Luca, A. P. 1980. The postcranial skeleton of *Heterodontosaurus tucki* (Reptilia, Ornithischia) from the Stormberg of South Africa. Palaeontologia Africana 25:151–180.

Scheyer, T. M. 2007. Skeletal histology of the dermal armor of Placodontia: the occurrence of 'postcranial fibro-cartilaginous bone' and its developmental implications. Journal of Anatomy 211:737–753.

Scheyer, T. M., and J. B. Desojo. 2011. Palaeohistology and external microanatomy of rauisuchian osteoderms (Archosauria: Pseudosuchia). Palaeontology 54:1289–1302.

Scheyer, T. M., and P. M. Sander. 2004. Histology of ankylosaur osteoderms: implications for systematics and function. Journal of Vertebrate Paleontology 24:874–893.

Scheyer, T. M., and P. M. Sander. 2007. Shell bone histology indicates terrestrial palaeoecology of basal turtles. Proceedings of the Royal Society B: Biological Sciences 274:1885–1893.

Scheyer, T. M., and P. M. Sander. 2009. Bone microstructures and mode of skeletogenesis in osteoderms of three pareiasaur taxa from the Permian of South Africa. Journal of Evolutionary Biology 22:1153–1162.

Scheyer, T. M., J. B. Desojo, and I. A. Cerda. 2014. Bone histology of phytosaur, aetosaur, and other archosauriform osteoderms (Eureptilia, Archosauromorpha). Anatomical Record 297:240–260.

Sereno, P. C. 1991. Basal archosaurs: phylogenetic relationships and functional implications. Journal of Vertebrate Paleontology 11:1–53.

Sereno, P. C., and A. B. Arcucci. 1990. The monophyly of crurotarsal archosaurs and the origin of bird and crocodile ankle joints. Neues Jahrbuch für Geologie und Paläontologie, Abhandlungen 180:21–52.

Taborda, J. R. A., I. A. Cerda, and J. B. Desojo. 2013. Growth curve of *Aetosauroides scagliai* Casamiquela 1960 (Pseudosuchia: Aetosauria) inferred from osteoderm histology, pp. 413–423 in S. J. Nesbitt, J. B. Desojo, and R. B. Irmis (eds.), Anatomy, Phylogeny, and Palaeobiology of Early Archosaurs and Their Kin. Special Publication 379. Geological Society, London.

Tsuihiji, T. 2005. Homologies of the transversospinalis muscles in the anterior presacral region of Sauria (crown Diapsida). Journal of Morphology 263:151–178.

Vickaryous, M. K., and B. K. Hall. 2008. Development of the dermal skeleton in *Alligator mississippiensis* (Archosauria, Crocodylia) with comments on the homology of osteoderms. Journal of Morphology 269:398–422.

Walker, A. D. 1961. Triassic reptiles from the Elgin area: *Stagonolepis*, *Dasygnathus* and their allies. Philosophical Transactions of the Royal Society London B: Biological Sciences 244:103–204.

Walker, A. D. 1964. Triassic reptiles from the Elgin area: *Ornithosuchus* and the origin of carnosaurs. Philosophical Transactions of the Royal Society London B: Biological Sciences 248:53–134.

Weinbaum, J. C. 2013. Postcranial skeleton of *Postosuchus kirkpatricki* (Archosauria: Paracrocodylomorpha), from the upper Triassic of the United States; pp. 525–553 in S. J. Nesbitt, J. B. Desojo, and R. B. Irmis (eds.), Anatomy, Phylogeny, and Palaeobiology of Early Archosaurs and Their Kin. Special Publication 379. Geological Society, London.

Witzmann, F. 2009. Comparative histology of sculptured dermal bones in basal tetrapods, and the implications for the soft tissue dermis. Palaeodiversity 2:e270.

Witzmann, F. 2010. Morphological and histological changes of dermal scales during the fish-to-tetrapod transition. Acta Zoologica 92:281–302.

Witzmann, F., and R. Soler-Gijón. 2008. The bone histology of osteoderms in temnospondyl amphibians and in the chroniosuchian *Bystrowiella*. Acta Zoologica 91:96–114.

Zittel, K. A. von. 1887–1890. Paläozoologie Band III. Vertebrata (Pisces, Amphibia, Reptilia, Aves). Handbuch der Paläontologie. Abteilung 1. Oldenbourg, Munich, 1890 pp.